

→ uranium-233 → thorium-229) has also been evaluated. The daughter contribution is less than 2 percent at 1 million years (CRWMS M&O 2000ea, Section 6.13.1.2). As such, daughter contributions to the neptunium-237 transport are relatively insignificant.

Colloid-Facilitated Transport Parameters—

Anthropogenic colloids may be produced from the waste or from potential repository construction and sealing materials. This was demonstrated in an experiment on simulated weathering of a high-level radioactive waste glass, where the amounts of plutonium and americium released from waste forms were orders of magnitude greater than their respective concentrations in the dissolved phase (Bates et al. 1992). Constraints on these types of colloids are described in Section 4.2.7 and are treated in *Waste Form Degradation Process Model Report* (CRWMS M&O 2000bm, Section 3.8). Relative to waste form colloids, natural colloid-facilitated transport is much lower and plays a minor role in releases from the repository (CRWMS M&O 2000ec, Section 6.6).

The association of radionuclides with colloids is modeled using two end-member representations: (1) reversible equilibrium exchange with the aqueous phase and (2) irreversible attachment. Radionuclides associated with colloids in either condition (reversible or irreversible) may be subject to size exclusion for fracture–matrix exchange. Colloids are excluded from moving from a fracture into matrix pores smaller than the colloid diameter. This tends to keep colloids (and the associated radionuclides) in the fractures, which leads to more rapid transport of the radionuclides. The chance of exclusion of a colloid from the matrix during fracture–matrix exchange is computed using a probabilistic method that considers different colloid-size and pore-size distributions (CRWMS M&O 2000ec, Section 6.2.1).

The description of reversible, colloid-facilitated radionuclide transport for the particle-tracking transport model used in performance assessment is quantified through two parameters (CRWMS M&O 2000ed, Section 6.1.4). One parameter defines the equilibrium partitioning of radionu-

clides between the aqueous phase and colloids. The other parameter is a retardation factor that captures the details of an equilibrium balance between colloid deposition and resuspension. The retardation factor in the colloid model abstraction applies to the transport through fractures. The distribution of retardation factors used is derived from C-Wells data for saturated-zone colloid transport (CRWMS M&O 2000ed, Section 6.2.5). The accessibility factors of colloids of different sizes were evaluated for different geological units (CRWMS M&O 2000ec, Table 3). The linear kinetic model of colloid filtration was used, with the forward kinetic coefficient directly computed (CRWMS M&O 2000ea, Section 6.16).

Colloid concentrations have been measured in several groundwater samples from Yucca Mountain and from other areas at the Nevada Test Site. The measured particle concentrations vary between 1.05×10^6 and 2.72×10^{10} particles per mL, with the lowest being for water from Well J-13 and the highest for water from Well U19q on Pahute Mesa (CRWMS M&O 2000ec, Section 6.2.2.2). These values are consistent with what has been reported in the literature for various groundwaters around the world.

4.2.8.2.3 Analogues for Unsaturated Zone Radionuclide Transport

Natural and anthropogenic sites around the world potentially provide sources of long-term data on the behavior of radionuclides and various metals that may serve as analogues to radionuclide transport at Yucca Mountain (CRWMS M&O 2000c, Section 3.11.12). In this section, some of the more important analogue sites for transport in the unsaturated zone are discussed; additional discussion is presented by *Natural Analogs for the Unsaturated Zone* (CRWMS M&O 2000bp).

Colloid Transport at the Nevada Test Site—

There is some field evidence for the occurrence of colloid-facilitated transport of radionuclides at or near the Nevada Test Site. In one case, migration of plutonium and americium, attributed to colloidal transport, was found more than 30 m (100 ft) downward through unsaturated tuff over the period of approximately 30 years below a low-level waste

site (Buddemeier and Hunt 1988, p. 536). In a saturated zone study at the Nevada Test Site, the isotopic ratio of plutonium-240 to plutonium-239 in groundwater showed that plutonium had been transported more than 1.3 km (0.8 mi) from an underground explosion cavity to a test well over a 30-year period, although plutonium is strongly sorbing at the Nevada Test Site and assumed to be immobile (Kersting et al. 1999). Filtration of groundwater samples from the test well indicated that the plutonium was on colloidal material. It is difficult to interpret the plutonium observed at the Nevada Test Site because it originated from an underground nuclear bomb test. The effects of the underground blast on the movement of plutonium are not fully understood.

Uranium Migration at Peña Blanca, Mexico— Since the 1980s, the Nopal I uranium deposit at Peña Blanca (see Figure 4-19b in Section 4.2.1) has been recognized as a natural analogue for the potential repository at Yucca Mountain. From the uranium–thorium age data, it appears that the primary transport of uranium occurred more than 300,000 years ago. Subsequently, there has been little redistribution of uranium-238 and uranium-235. The 300,000-year stability of uranium-235, uranium-238, thorium, and protactinium in fracture-fill minerals has survived recent hydrologic disturbances from surface water infiltration of the fractures. Recent data indicate that the geochemical system at Nopal I restricts actinide mobility in the unsaturated environment. By analogy, the tuffs at Yucca Mountain should have similar retentive properties and impede the mobility of oxidized uranium.

The McDermitt Caldera uranium deposits and other uranium deposits in northwestern Nevada and southeastern Oregon, together with many other uranium sites and contaminated sites worldwide, are discussed in *Natural Analogs for the Unsaturated Zone* (CRWMS M&O 2000bp). These natural analogue studies build confidence in the flow and transport process models.

Artifact Preservation at Akrotiri, Greece— Akrotiri, Greece has silicic volcanic rocks, a dry climate, and oxidizing, hydrologically unsaturated subsurface conditions that are similar to those at

Yucca Mountain. The Minoan eruption, an eruption of volcanic ash 3,600 years ago, buried bronze and lead artifacts under 1.5 to 2.0 m (5 to 6 ft) of ash. Researchers looked for plumes of copper, tin, and lead beneath the artifacts by selectively leaching packed earth and bedrock samples that were collected beneath the artifacts. Little of the bronze material had been transported away from the artifacts. Copper and lead plumes were found beneath the artifacts, but neither was detected below a depth of about 45 cm (18 in.). The Akrotiri study shows preservation of artifacts for a long period of time in an oxidizing environment, indicating that unsaturated systems in arid environments may provide favorable sites for geologic disposal of radioactive waste (Murphy et al. 1998).

4.2.8.3 Unsaturated Zone Flow and Transport Process Models

Section 4.2.1 described seepage into the drifts. In this section, additional understanding of flow diverted around drifts and of condensate shed away from the drifts is discussed in Section 4.2.8.3.1. After the radionuclides are transported to the tuff units below the potential repository horizon, the current understanding of the impact of perched water is summarized in Section 4.2.8.3.2. The modeling results on the temporal and spatial distributions of particle released from the potential waste emplacement drifts to the water table are described in Section 4.2.8.3.3. Alternative conceptual processes and limitations and uncertainties are discussed in Sections 4.2.8.3.4 and 4.2.8.3.5, respectively.

4.2.8.3.1 Seepage Diversion and Condensate Shedding

Both the advective and diffusive transport processes determine the rates of radionuclide releases in the drift and transport below the drift. With percolation flux below the seepage threshold and limited amount of seepage flux available (as described in Section 4.2.1.4.2) for advective transport, the release rate is sensitive to enhanced diffusive transport (CRWMS M&O 2000a, Sections 3.6.3.1 and 5.2.5.1). Figure 4-116 is a conceptual sketch that illustrates the concepts of the possible diffusion-dominated flow field or the

advection-dominated flow field in the zone below the drift, discussed in the following paragraphs. The results of analyses of drift seepage for performance assessment (CRWMS M&O 2000bx, Section 6.6.6) indicate that the drift acts as a barrier to downward percolation and that the region below the drift is a drier shadow zone, as illustrated in Figure 4-117. More recent modeling and analysis of the drift shadow zone are presented in Volume 1, Sections 11.2.1 and 11.3.1 of *FY01 Supplemental Science and Performance Analyses* (BSC 2001a).

As long as waste packages are warm enough to heat the air in emplacement drifts, the heat will tend to desaturate the rock around the drifts and redistribute the water. If liquid water is boiled away near the drift during the thermal period, little or no seepage into the drifts is expected. The functioning of the hot and dry barrier is illustrated in Figure 4-118, based on the thermal-hydrologic model and the thermal seepage model (CRWMS M&O 2000ci, Section 6.11.2; BSC 2001o, Section 6.3.5). The drift shadow zone remains relatively dry during the thermal period. The percolation and

seepage after the waste heat decays will be essentially equal to the preemplacement rates if the hydrologic properties and conditions are not significantly altered.

4.2.8.3.2 Lateral Flow Associated with Perched Water Bodies

This section summarizes the effects of perched water bodies on the unsaturated flow field below the potential repository (CRWMS M&O 2000c, Section 3.7.3.3). The geological setting of perched water bodies was presented in Section 4.2.1.1.2 (and illustrated there in Figure 4-7). The occurrence of perched water indicates that the base of the Topopah Spring welded hydrogeologic unit and the zeolitic layers within the Calico Hills nonwelded hydrogeologic unit may serve as barriers to vertical flow and cause lateral diversion of flow. The spatial distribution of low-permeability zeolites has been modeled using mineralogic and petrologic data from several boreholes and is presented in *Integrated Site Model Process Model Report* (CRWMS M&O 2000i).

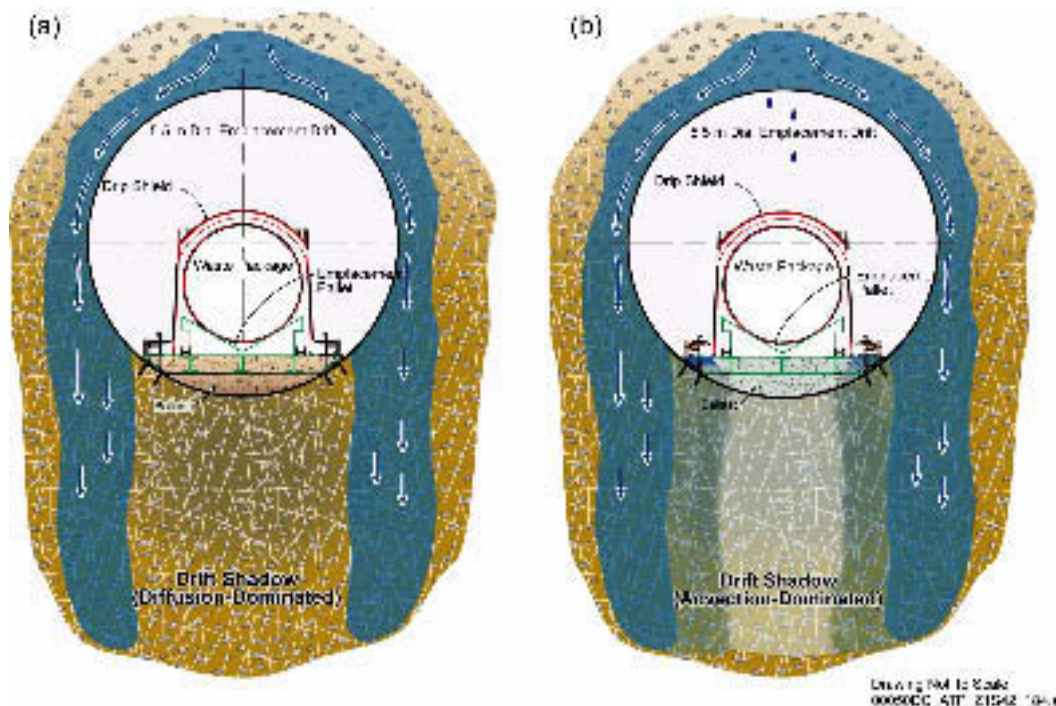


Figure 4-116. Schematic Diagram of Diffusion Barriers in Invert and Drift Shadow Zone

(a) Schematic with diffusion barriers enhanced by seepage diversion and drip shield. (b) Schematic with diffusion barriers influenced by surface diffusion and advective transport. See also Section 2.4.1, Figures 2-71 and 2-72 for the invert structure selected for the potential emplacement drift.

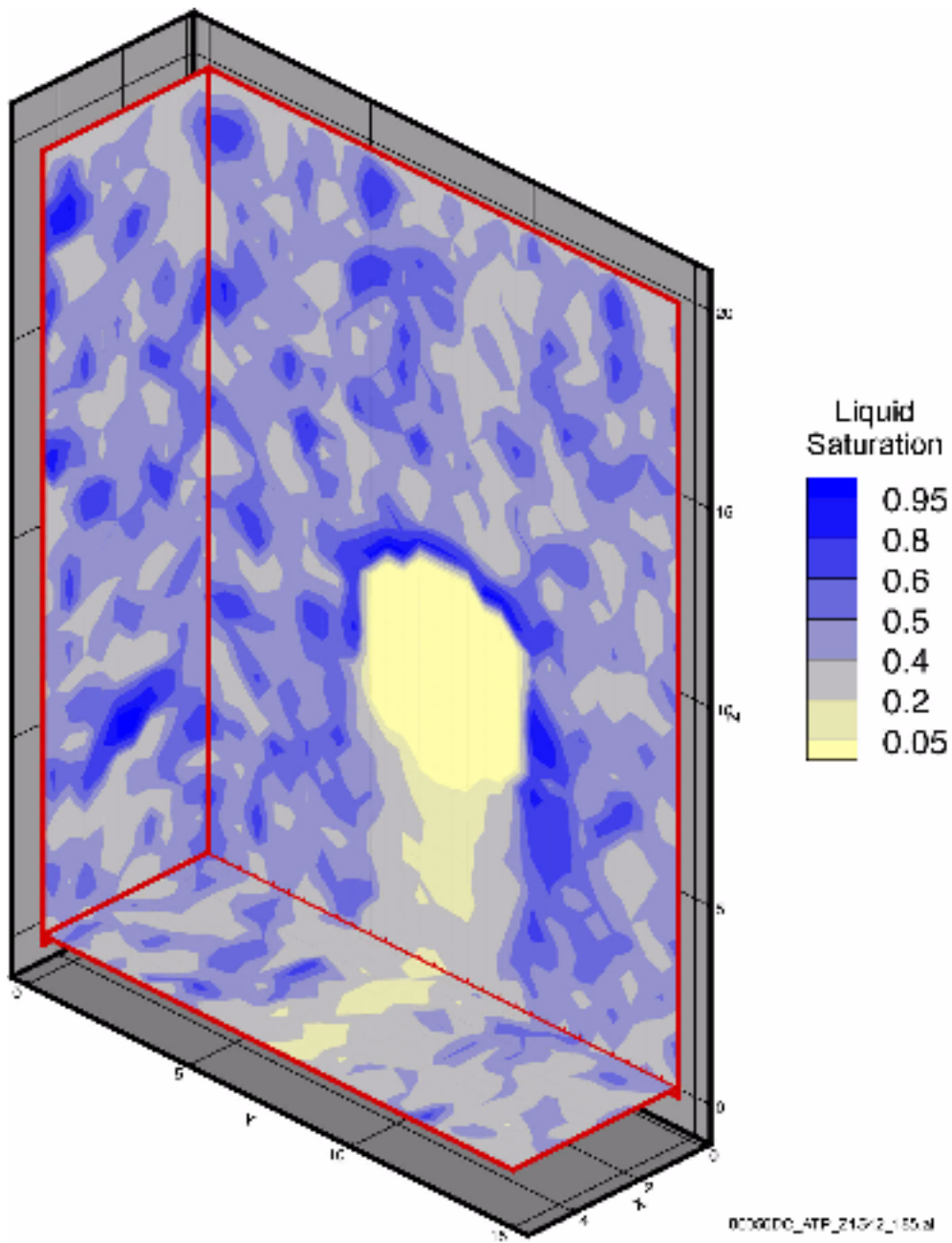


Figure 4-117. Saturation Profiles around a Drift from a Seepage Model for Performance Assessment
Source: CRWMS M&O 2000bx, Figure 5.

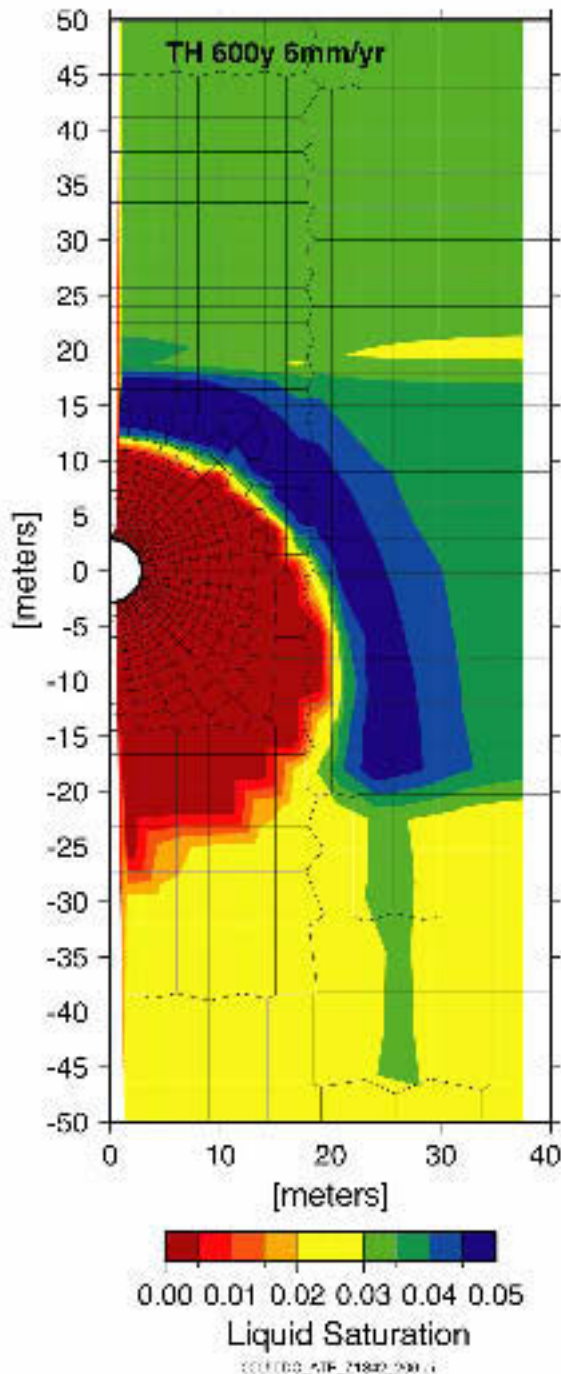


Figure 4-118. Condensate Shedding during the Thermal Period
Source: BSC 2001o, Figure 32b.

Figure 4-13 (see Section 4.2.1.2.10) shows the modeled distribution of zeolites for layers within the lower Topopah Spring welded and the upper Calico Hills nonwelded hydrogeologic units. Areas with 3 percent or less zeolite by weight are considered vitric, or unaltered.

Zeolites within the Calico Hills nonwelded hydrogeologic unit are prevalent in the northern and eastern portion of the model domain (Figure 4-13). The areal extent of the vitric region diminishes with depth and is considered to be largely confined to the fault block bounded on the north and east by the Sundance and Ghost Dance faults, respectively, and in the west by the Solitario Canyon fault. The northern half of the potential repository area is underlain by the predominantly zeolitic Calico Hills nonwelded hydrogeologic unit, while the southern half is underlain by the predominantly vitric upper portion of the Calico Hills nonwelded hydrogeologic unit. However, below the vitric Calico Hills nonwelded hydrogeologic unit (yet above the water table) are nonwelded portions of the Prow Pass, Bullfrog, and Tram tuffs that are pervasively altered to zeolites. Thus, there appears to be no direct vertical pathway from the potential repository horizon to the water table that does not intersect zeolitic units, except perhaps within fault zones.

The spatial distributions of vitric and zeolitic material within the Calico Hills nonwelded hydrogeologic unit, along with the characterization of the basal vitrophyre of the Topopah Spring welded hydrogeologic unit, are important for understanding the distribution of perched water and for determining potential flow paths for radionuclides. Figure 4-119 shows a perspective view of the extent of perched water in the lower Topopah Spring welded hydrogeologic unit based on three-dimensional simulations with mean, present-day infiltration rates.

Performance assessment analyses, described in *Analysis of Base-Case Particle Tracking Results of the Base-Case Flow Fields (ID: U0160)* (CRWMS M&O 2000cb, Sections 6.2.1 and 6.2.2), considered the particle breakthrough locations and times resulting from two perched water conceptual models. Figure 4-120 shows the particle-break-

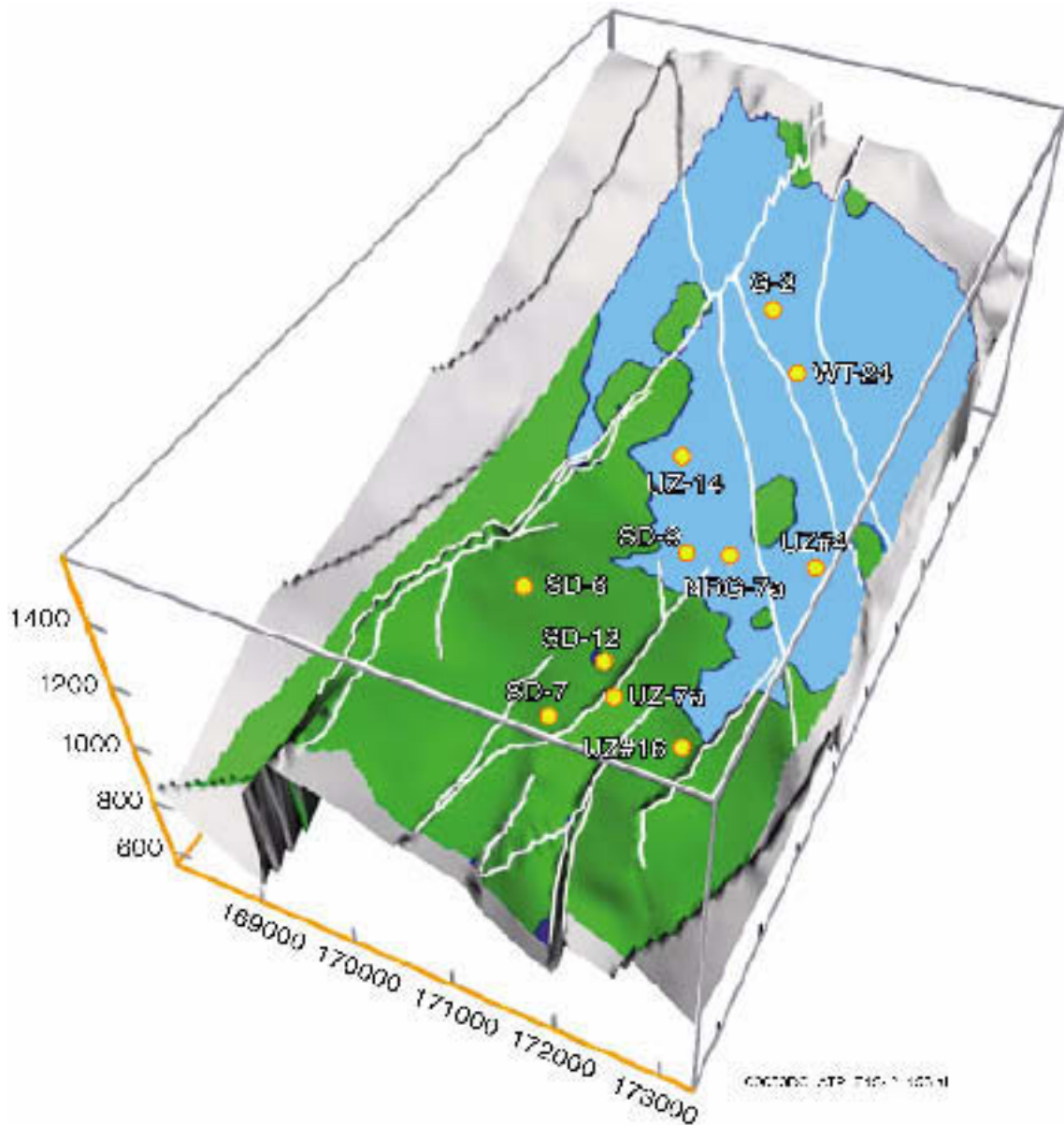


Figure 4-119. Perched Water at the Base of the Topopah Spring Welded Hydrogeologic Unit

Figure based on a simulation with present-day mean infiltration rates. Blue indicates 100 percent liquid saturation (perched water) within fractures; green indicates less than 100 percent fracture liquid saturation. Elevation is given in meters; horizontal coordinates are Nevada State Plane, Easting. Source: CRWMS M&O 2000bw, Figure 6-9.

through locations at the water table for an advective tracer (no diffusion, sorption, or dispersion) released uniformly as a pulse in the outlined potential repository region using the mean infiltration case for the glacial-transition climate. Both perched-water models show a large amount of lateral diversion of particles beneath the northern portion of the potential repository. Many of the diverted particles are concentrated in faults, which, based on the simulated fault properties, channel water to the water table. Perched-water model #2 (permeability barrier, unfractured zeolite model) shows more lateral diversion in the southern portion of the potential repository area because of the absence of enhanced fracture permeability in zeolitic units of the Calico Hills nonwelded hydro-

geologic unit. Perched-water model #1 (permeability barrier, fractured zeolite model) shows breakthrough over a large area in the southern half of the potential repository footprint because of enhanced fracture permeability in zeolitic portions of the Calico Hills nonwelded hydrogeologic unit in areas where perched water is absent.

Additional results from modeling studies that investigate flow distribution within the Calico Hills nonwelded hydrogeologic unit, perched water occurrence, and the effects on flow and transport of major faults below the potential repository horizon are summarized in Section 4.2.1.3.

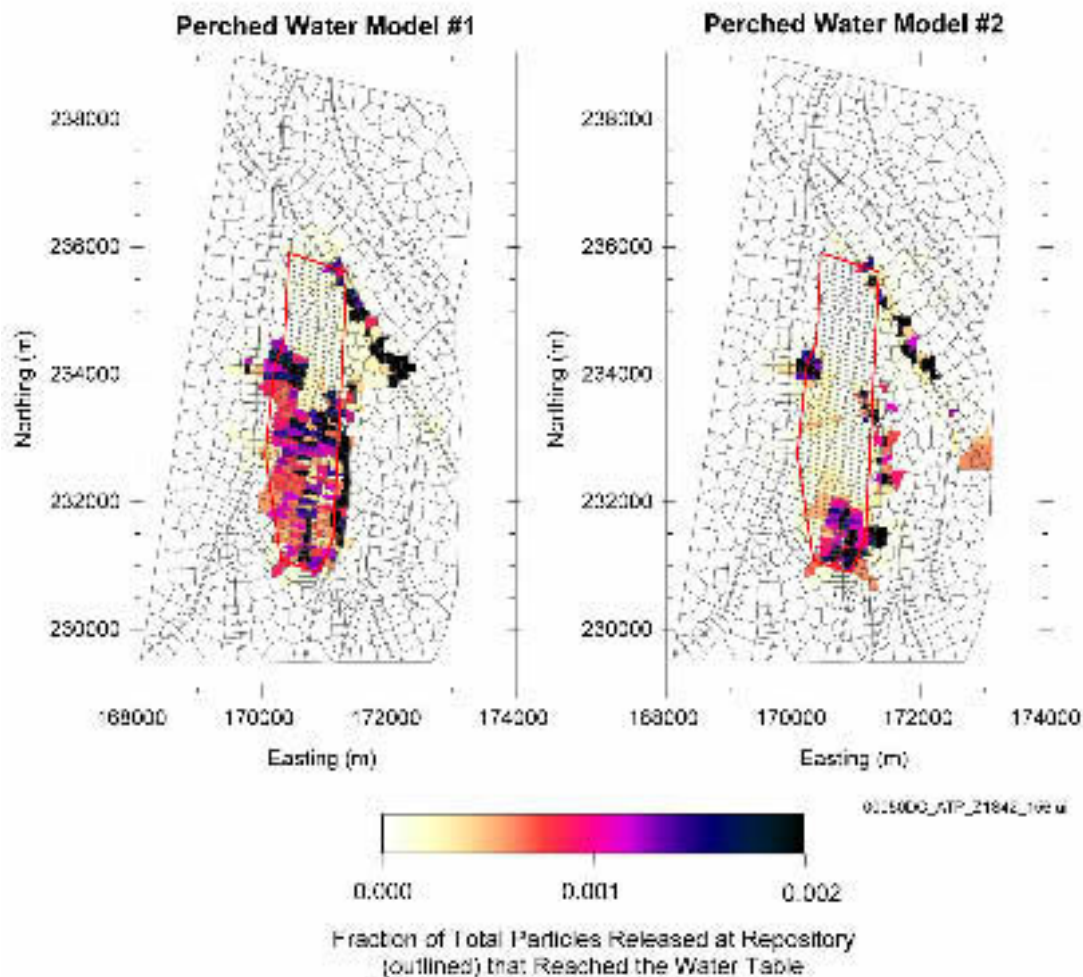


Figure 4-120. Locations of Particle Breakthrough at the Water Table for the Mean Infiltration, Glacial-Transition Climate Using Two Perched Water Models

Source: CRWMS M&O 2000c, Figure 3.7-16.

4.2.8.3.3 Flow and Transport in Geological Layers below the Potential Repository

In addition to unsaturated zone flow processes, radionuclide migration depends on transport properties, colloid transport mechanisms, and the geochemical environment. The relationship of other models and data feeds to the unsaturated zone transport model are schematically illustrated in Figure 4-121. Most of the model assumptions and approaches are similar to the corresponding unsaturated zone flow model components. The integrated flow and transport model is presented more fully in *Unsaturated Zone Flow and Trans-*

port Model Process Model Report (CRWMS M&O 2000c, Section 3.11).

4.2.8.3.3.1 Transport of Nonsorbing and Sorbing Radionuclides through the Hydrogeologic Units

For transport assessment, nonsorbing and weakly sorbing radionuclides with long half-lives are the primary concern. In sensitivity analyses, processes, properties, and model results are presented for the representative radionuclides: technetium-99 (nonsorbing), neptunium-237 (moderately sorbing), plutonium-239 (strongly sorbing), and its long-lived daughter uranium-235 (moderately

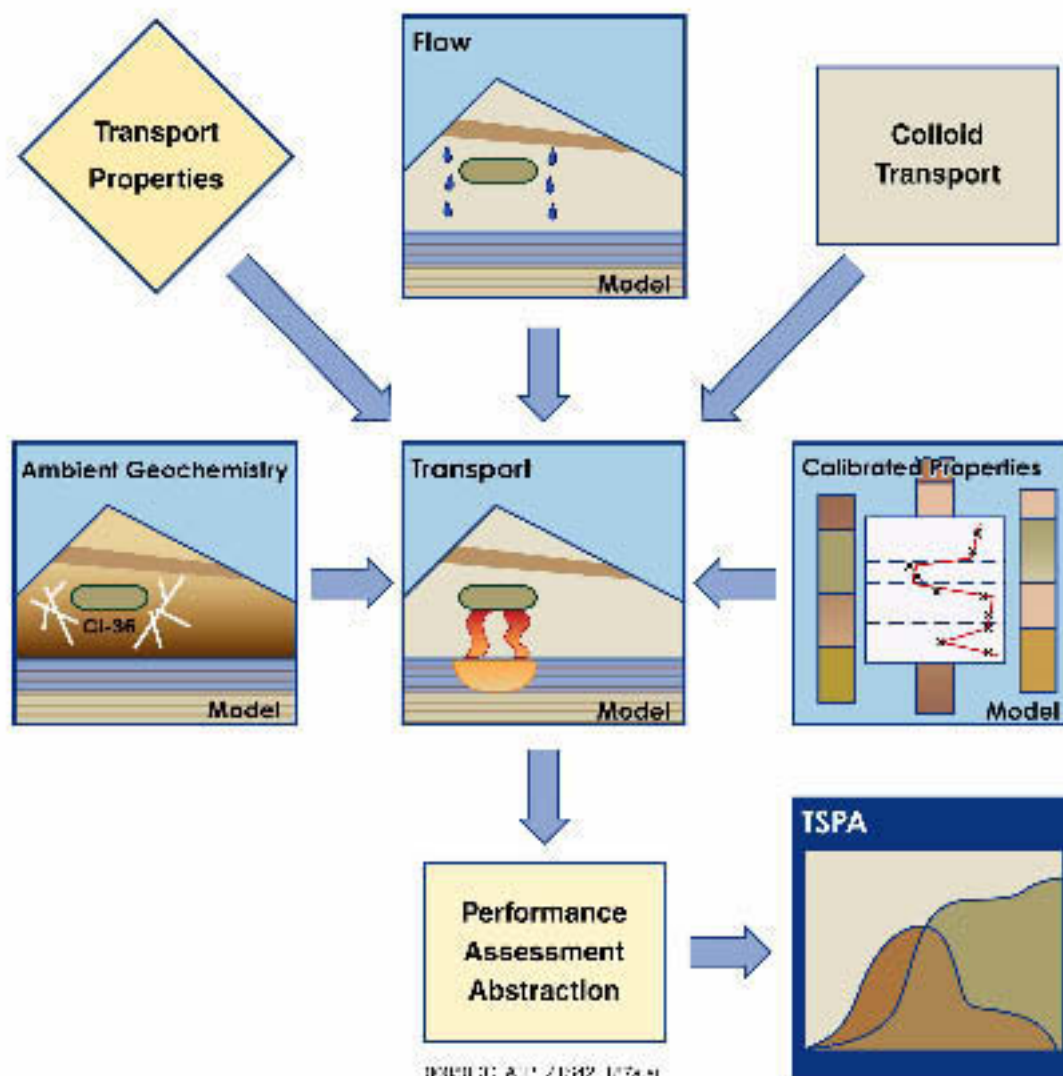


Figure 4-121. Relationships of Other Models and Data Inputs to the Unsaturated Zone Transport Model
Source: CRWMS M&O 2000c, Figure 3.11-2.

sorbing). In these analyses, the radionuclides are released continuously at the top of the model domain (which coincides with the location of the potential repository), and the contaminant distribution is monitored over time for different percolation rates. In TSPA, the full inventory of radionuclides and their daughters are included to assess the total radioactivity distribution.

Flow in the zeolitic portions of the Calico Hills nonwelded hydrogeologic unit is judged to be dominated by fracture flow. In some welded and zeolitic layers, the matrix permeability is insufficient to carry the net infiltration, which implies that a portion of the percolation is likely to be carried by fractures (CRWMS M&O 2000c, Section 3.6.3.1). In vitric portions of the Calico Hills nonwelded hydrogeologic unit, matrix and fracture permeabilities are on the same order of magnitude; therefore, these layers behave as porous (rather than fractured) media, and flow is matrix-dominated. Fracture flow in the Topopah Spring welded hydrogeologic unit will be strongly attenuated,

transport velocities greatly reduced, and contact of dissolved radionuclides with the rock matrix enhanced by the slower velocities, longer contact time, and stronger fracture–matrix interaction, which leads to more retardation for sorbing radionuclides. Based on current understanding, the Prow Pass and Bullfrog tuffs are heterogeneous, with some zeolitic layers and some devitrified and unaltered layers (CRWMS M&O 2000c, Section 3.11.4).

4.2.8.3.2 Two-Dimensional Radionuclide Transport at Representative Borehole Locations

The effect of geologic layers on radionuclide migration below the potential repository is illustrated in Figure 4-122, which illustrates, conceptually, flow and transport processes in two representative hydrogeologic profiles. Borehole USW UZ-14 is located in the northern part of the potential repository site, while borehole USW SD-6 is located in the southern part. Narrow-width

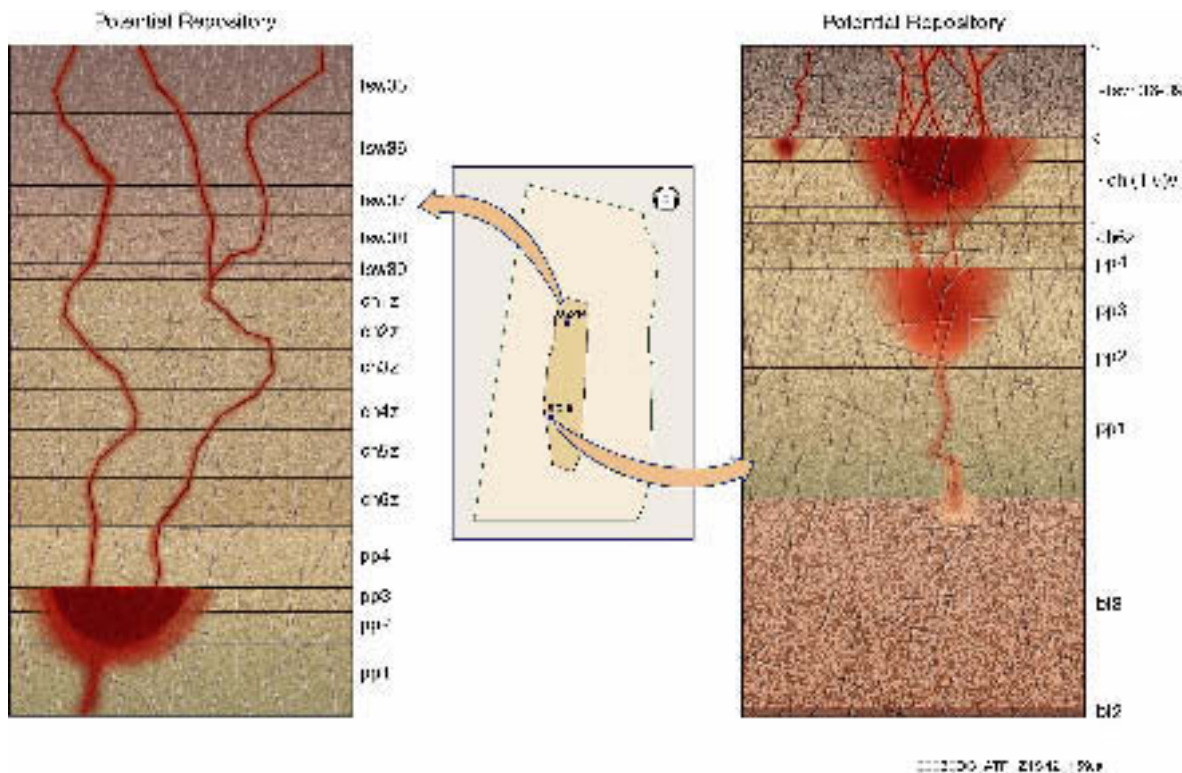


Figure 4-122. Flow and Transport in Two Representative Unsaturated Zone Hydrogeologic Profiles
Source: CRWMS M&O 2000c, Figure 3.11-3.

cross-sectional (two-dimensional) models were developed at each of these locations. As radionuclides leave the potential repository, they could quickly migrate through the Topopah Spring welded hydrogeologic layers with limited matrix diffusion and sorption. Vitric layers could retard migration because of the matrix-dominated flow in these layers, while radionuclides could quickly pass through zeolitic layers due to the fracture-dominated flow (CRWMS M&O 2000c, Section 3.11.4).

The difference in the capacity to retard radionuclides between vitric and zeolitic tuffs is illustrated in Figure 4-123 for two-dimensional simulations with a percolation rate of 6 mm/yr (0.24 in./yr) (close to the mean present-day rate). At 10,000 years, the breakthrough to the water table for the moderately sorbing neptunium-237 occurs through zeolitic layers (in a cross section including borehole USW UZ-14) and does not occur through mainly vitric layers (in a cross section including borehole USW SD-6). Transport of other radionuclides through individual layers is summarized in *Unsaturated Zone Flow and Transport Model Process Model Report* (CRWMS M&O 2000c, Section 3.11.5). The two-dimensional simulations do not allow lateral diversion in the third dimension.

4.2.8.3.3.3 Three-Dimensional Mountain-Scale Radionuclide Transport

In the three-dimensional model (CRWMS M&O 2000c, Section 3.11.6), the spatial distribution of percolation is heterogeneous with perched water and faults affecting the percolation distribution below the potential repository. Modeling of radionuclide transport using the mountain-scale three-dimensional grids (CRWMS M&O 2000ea, Sections 6.11 to 6.16) were performed, and breakthrough is described by a normalized release rate, R , (i.e., the ratio of radionuclide mass release rates at the water table versus that at the potential repository).

The normalized release rate for nonsorbing technetium-99 depends strongly on the infiltration rate (Figure 4-124). As the infiltration rate increases from lower-bound to mean present-day level, the

t_{10} time, defined as the time at which $R = 0.1$, decreases from about 10,000 years to about 300 years. The t_{50} , the time at which $R = 0.5$, decreases from about 45,000 years to about 4,000 years. The upper-bound infiltration rate further reduces t_{10} and t_{50} . The maximum attainable normalized release rate decreases with the infiltration rate because lower infiltration results in lower velocities and slower transport, thus higher radioactive decay.

From t_{10} and t_{50} values, the moderate sorption and resulting retardation of neptunium-237 is sufficient to increase the time to reach the water table by a factor of about 40. The $R = 1.0$ limit is not achieved within the simulation period. At 1 million years, R is 0.98, 0.86, and 0.42 for the upper-bound, mean, and lower-bound infiltration rates, respectively.

The normalized release rate for strongly sorbing plutonium-239 never reaches the 0.1 level, even after 1 million years of continuous release. The picture changes dramatically, however, if the daughter contributions to the release rate at the water table are accounted for in the computations. Given the half-life of plutonium-239 and the much longer half-life of uranium-235, the daughter contributions can become important. The relative flux fractions, M_R , are also shown in Figure 4-124. The plutonium contribution to the release rate starts declining rapidly after 1,000 years, and uranium-235 is by far the dominant species after 10,000 years (CRWMS M&O 2000ea, Section 6.14.1.2). After 1,000 years, the release at the water table consists mostly (over 95 percent) of uranium-235 under the lower-bound, present-day infiltration rate. The protactinium-231 contribution is negligible because of the very long half-life of uranium-235.

Direct comparison of perched-water hydrogeochronology and modeled radionuclide breakthrough times is hindered by the differences in the flowpaths of the water in both cases and the role and magnitude of retardation of the different radionuclides in the transport models. There are, nonetheless, some inferences that can be drawn about the percolation flux rates in the deep unsaturated zone and the style of flow in that region that

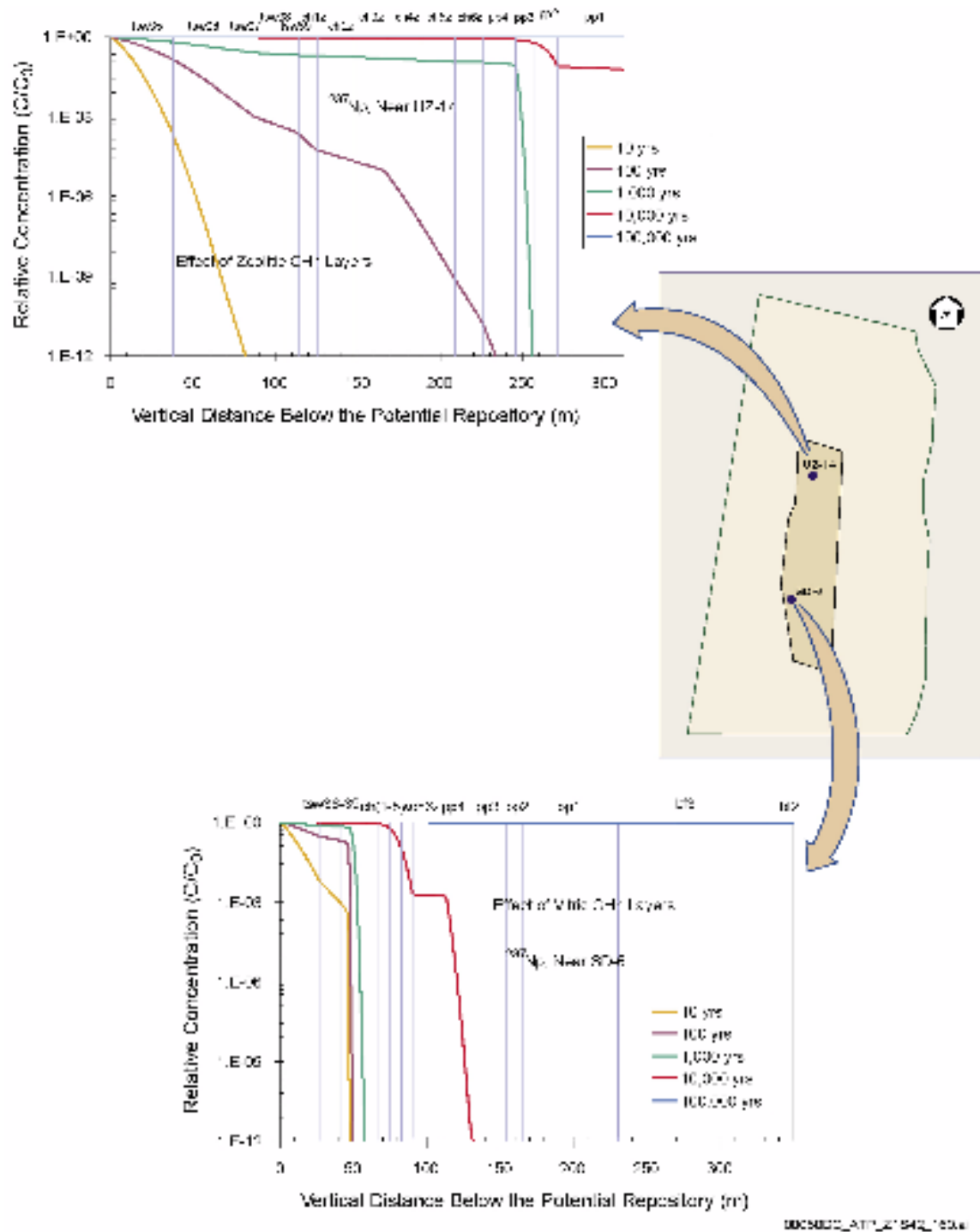


Figure 4-123. Comparison of Transport Characteristics in USW UZ-14 and USW SD-6

The data shown in this figure are based on a model that is appropriately conservative for TSPA analysis and not intended to represent expected breakthrough of radionuclides of the water table. Source: CRWMS M&O 2000c, Figure 3.11-4.

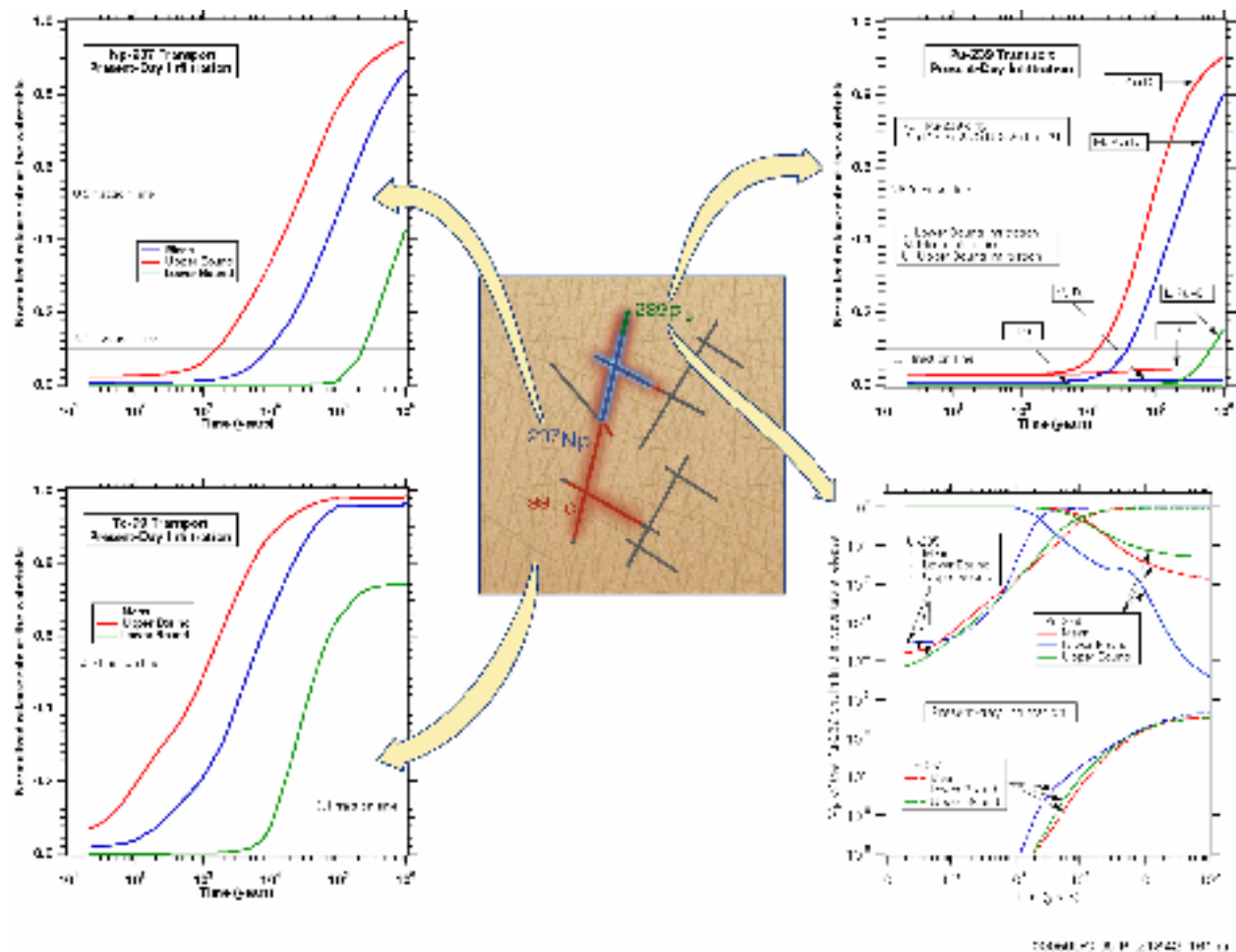


Figure 4-124. Normalized Release Rate and Dependence of Technetium-99 Transport on Infiltration Rates
The data shown in this figure are based on a model that is appropriately conservative for TSPA analysis and not intended to represent expected breakthrough of radionuclides at the water table. Source: CRWMS M&O 2000c, Figure 3.11-5.

are useful in supporting the understanding of unsaturated zone transport.

Perched water is a mixture of old and young water, with the oldest water perhaps being the product of flow during past wetter climates and the youngest water being the result of fast fracture flow. The chlorine-36 analyses of perched water indicate ages ranging from 2,000 to 12,000 years, in general agreement with the carbon-14-based ages (BSC 2001r, Section 6.6.3.6; Yang, Rattray et al. 1996). Variation in ages from place to place in the perched water bodies indicates incomplete mixing of old and young water. Pore water near fault zones (borehole UZ#16) is sometimes apparently some-

what younger than the water in nearby perched-water bodies (Yang, Rattray et al. 1996).

Major ion concentrations and uranium isotope data indicate that the perched-water bodies formed from water different from water in the matrix of the host rock and that little equilibration has taken place between these waters (BSC 2001r, Section 7.5). This suggests that perched water arrived at its present location by fracture flow in a flow system in which there was little liquid exchange between the fractures and the matrix. This observation supports the dual permeability model used in evaluating unsaturated zone transport.

The apparent radionuclide transport times from the repository horizon to the water table average about 5,000 years (CRWMS M&O 2000c, Section 3.11.8), falling at about the median age of perched water (BSC 2001s, Section 6.2.1.2). Although the flowpaths and details of radionuclide retardation are different, the fracture-dominated dual-permeability flow mechanism is comparable, and the youngest perched water is not much younger than the predicted breakthrough times. The hydrogeochronology of the perched water therefore permissively supports the modeled breakthrough times by demonstrating slow percolation in the deep unsaturated zone and the geochemistry of the fracture and matrix water supports the dual permeability model used in the breakthrough modeling.

Where transported radionuclides intersect perched water, the role of the perched-water bodies in transport includes the dilution of radionuclides and delay associated with residence time in the perched-water bodies. The residence times and subsequent transport flowpaths are represented by two conceptual models, one representing vertically downward flow and another representing lateral diversion to faults and subsequent rapid downward flow to the water table (BSC 2001s, Section 6.5.3.2). These are known as the flow-through and flow-by models. The flow-through model is used in performance assessment because it is slightly faster and therefore more conservative.

Results of the three-dimensional simulation indicate that flow is diverted above the zeolitic Calico Hills nonwelded hydrogeologic unit and that radionuclides move slowly through the perched water to faults and to the vitric Calico Hills nonwelded hydrogeologic unit. In the three-dimensional model, transport is controlled by faults, especially at the early times (approximately 100 years). The Ghost Dance (southern splay), Sundance, and Drill Hole Wash faults are the main transport-facilitating features, providing fast pathways to the water table (CRWMS M&O 2000ea, Section 6.12.2.2). The main Ghost Dance fault does not play an important role in transport at the bottom of the Topopah Spring welded hydrogeologic unit, as the technetium-99 does not reach the fault at this level even after 100,000 years (CRWMS M&O 2000ea, Section 6.12.2.2). This fault is more important at

the water table, where it acts as a barrier to lateral transport while facilitating downward migration into the water table.

The transport pattern illustrated in Figure 4-125 indicates that radionuclide transport to the groundwater is expected to be faster in the southern part of the potential repository block, where it is also areally concentrated. There are several reasons for this. First, the rates and direction of water flow dictate the advective transport pattern, and the maximum water flow within the footprint of the potential repository is in its southern part in perched water model #1. Second, the presence of the highly conductive faults (e.g., Splay G of the Solitario Canyon fault and the Ghost Dance fault splay) act as the venue for fast transport, despite the fact that the vitric Calico Hills nonwelded hydrogeologic unit behaves as a porous medium (with relatively lower water velocities). These faster transport pathways may be facilitated by flow focusing in the vitric Calico Hills nonwelded hydrogeologic unit, which has a funnel-shaped distribution in the south. Third, the low-permeability zones at the Topopah Spring welded–Calico Hills nonwelded hydrogeologic unit interface in the northern part of the potential repository, act as barriers to water drainage, and lead to low water velocities and the presence of perched water bodies. Radionuclides move slowly through the perched water before reaching the underlying conductive zeolitic Calico Hills nonwelded hydrogeologic unit, hence the delay in transport. Radionuclide breakthrough at the water table occurs before 1,000 years and over a large area by 10,000 years in the southern part of the potential repository block.

4.2.8.3.3.4 Three-Dimensional Mountain-Scale Transport of Plutonium True Colloids

Plutonium, a major nuclear fuel element, can be present as a waste-form colloid (i.e., true or intrinsic colloid as elemental particle). The waste-form colloids will play a more significant role than natural colloids as pseudocolloids with radionuclides adsorbed to the naturally occurring fine particles (CRWMS M&O 2000ec, Section 7). Colloid size has an important effect on transport,

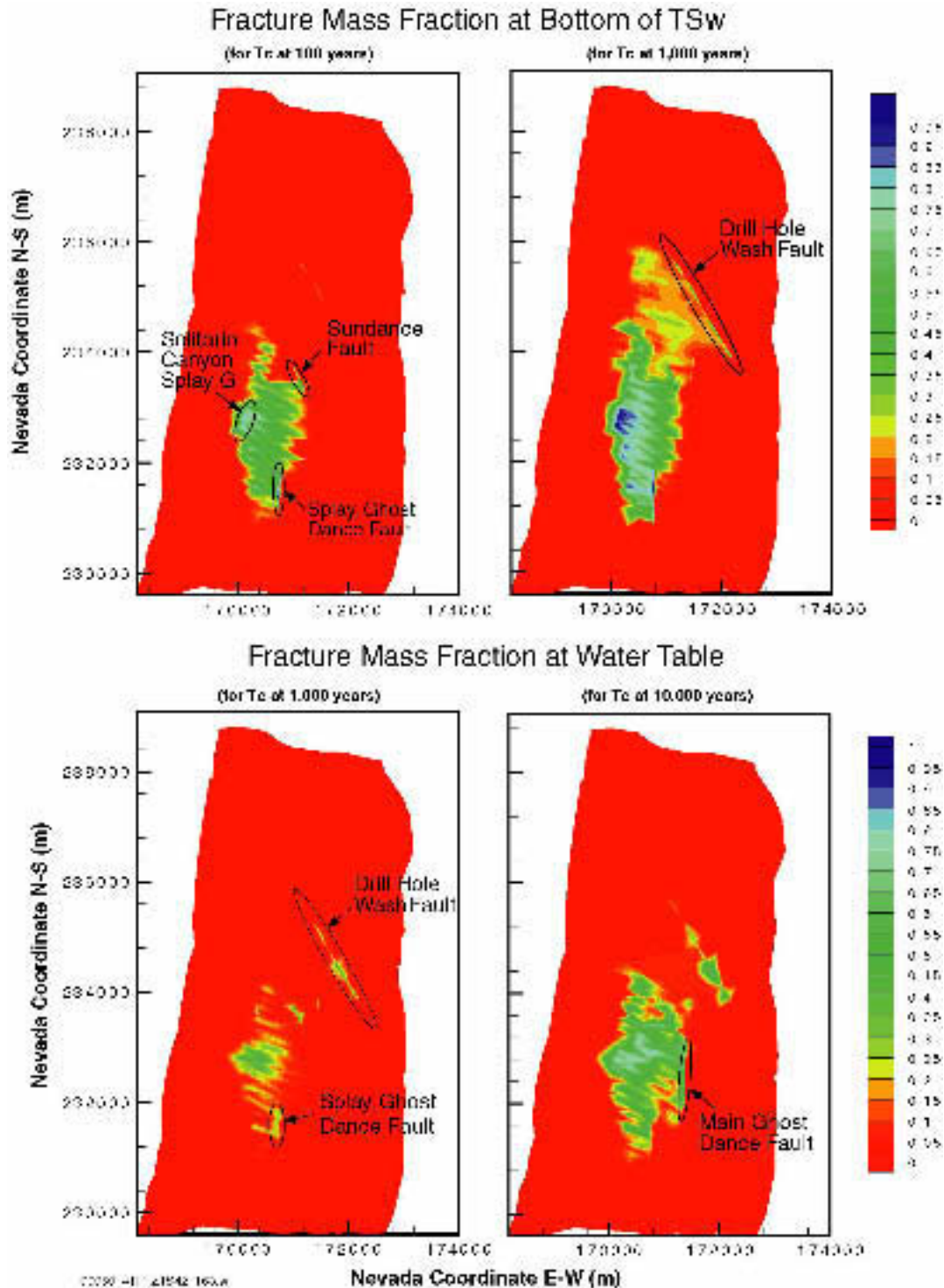


Figure 4-125. Normalized Mass Fraction Distribution of Technetium-99 in Fractures at the Bottom of the Topopah Spring Welded Hydrogeologic Unit and at the Water Table

The data shown in this figure are based on a model that is appropriately conservative for TSPA analysis and not intended to represent expected breakthrough of radionuclides at the water table. Source: CRWMS M&O 2000c, Figure 3.11-6.

and the size exclusion (inability of larger colloids to move into the matrix) results in enhanced transport to the groundwater. Smaller colloidal particles can diffuse more easily into the matrix, and their transport is thus more retarded. Size exclusion at the interfaces of different geologic units leads to colloid concentrations that can be significantly higher than that in the water released from the potential repository (CRWMS M&O 2000ea, Section 6.16). These high concentrations are observed behind (i.e., they do not penetrate) the interfaces because the large-size colloids cannot move across the interface.

4.2.8.3.4 Alternative Conceptual Approaches

The alternative conceptual processes for unsaturated flow below the potential repository horizon, as described in Section 4.2.1.3.4, have the same large impacts on the unsaturated zone transport. These alternative processes include episodic flow within the Topopah Spring welded hydrogeologic unit, flow through the perched water into the Calico Hills nonwelded unit without significant lateral diversion, and faults in the Calico Hills unit and below having low permeabilities. The conservatism and optimism associated with the advective transport are similar to the discussions in Section 4.2.1.3.4 and are not reiterated in this section.

Drift Shadow—If the shadow zone of drier conditions exists below the drift, the advective and diffusive transport will be greatly reduced in the vicinity of the radionuclide release points, as illustrated in Figures 4-116 to 4-118. Omitting the shadow process from the unsaturated zone transport model results in a conservative evaluation. A realistic representation, with drift-scale processes below the drift taken into account, would likely result in performance analyses that indicate more retardation of radionuclide transport in the unsaturated zone. More recent modeling and analyses, which show that the drift shadow may increase the radionuclide transport time from the repository horizon to the water table by several orders of magnitude, are presented in Volume 1, Sections 11.2.1 and 11.3.1 of *FY01 Supplemental Science and Performance Analyses* (BSC 2001a).

Matrix Diffusion—Some previous hydrologic models of Yucca Mountain have ignored the effects of matrix diffusion, an assumption that is very conservative because it ignores the interaction between water in fractures and the rock matrix, particularly in unwelded tuffs. This results in unrealistically fast predictions of transport. The available analyses of Alcove 1 infiltration tests indicate that the inclusion of matrix diffusion is important in interpreting the data and in validating the models. Ongoing testing and modeling of the Alcove 8 to Niche 3 Cross-Drift test can further validate the importance of matrix diffusion. While neglecting matrix diffusion is conservative, the alternative process model with no matrix diffusion is not realistic. In the TSPA-SR abstraction, matrix diffusion is explicitly incorporated and modeled (CRWMS M&O 2000c, Section 3.11.13.1).

4.2.8.3.5 Uncertainties and Limitations

The uncertainties and limitations for unsaturated flow, as described in Section 4.2.1.3.5—in climate, hydrologic properties in lower tuff units, geochemical analyses, and numerical approaches—are also applicable to unsaturated zone transport. In this section, uncertainties and limitations associated with field testing are first discussed, followed by evaluations of transport properties.

4.2.8.3.5.1 Uncertainties and Limitations for Field Testing in Lower Hydrogeologic Units

The field tests in construction water monitoring and liquid release testing are mainly limited to the tuff units accessible from the Exploratory Studies Facility, in and above the middle nonlithophysal zone of the Topopah Spring welded hydrogeologic unit. Ongoing tests along the Cross-Drift are generating additional data for the lower lithophysal unit, with additional tests in the lower nonlithophysal and the western part of the potential repository block planned. Uncertainties about transport below the drift can be reduced with relevant data collected.

The unsaturated zone transport test site at Busted Butte is in a distal extension of the vitric Calico Hills nonwelded hydrogeologic unit. The site-

specific information about the zeolitic Calico Hills nonwelded hydrogeologic unit is based on borehole cores. The uncertainties and limitations are being assessed by comparing tests in fractured units and in vitric units to demonstrate that core-scale data are adequate for site-scale assessment.

4.2.8.3.5.2 Uncertainties and Limitations in Transport Properties

Many conservative approximations are used in the performance assessments, leading to overestimation of radionuclide transport. Conservative assignments of transport parameters, potentially overconservative alternative models, and potentially optimistic (nonconservative) approaches all contribute to uncertainties in the assessment of transport processes in the unsaturated zone. In addition to the diffusion processes discussed in Section 4.2.8.3.4, some of the uncertainties and limitations of other flow and transport processes are further discussed below.

Matrix Sorption—The experimentally determined K_d values are mostly from batch experiments using crushed tuff under saturated conditions. These saturated conditions are not representative for ambient conditions in the unsaturated zone. The crushed rock tests can overestimate sorption, and fine particles generated in grinding can lead to irreproducible or high K_d values (CRWMS M&O 2000ea, Section 6.1.3.1). Measurements of tracer penetration into unsaturated core-size solid tuff samples can generate K_d values that are more directly related to processes of transport through fractured blocks observed in the field (CRWMS M&O 2000bu, Section 6.4).

Rate-Limited Sorption—Rate-limited sorption could be important, especially for fluid–radionuclide–rock systems with large sorption potential. Breakthrough curves for neptunium-237 transport in tuffs from the column experiments can only be analyzed by considering rate-limited sorption (Viswanathan et al. 1998, p. 267). This result indicates the existence of rate-limited sorption under flowing conditions. Nonlinear and irreversible sorption are also evident from the diffusion and transport studies in *Unsaturated Zone and Saturated Zone Transport Properties (U0100)*

(CRWMS M&O 2000eb, Sections 6.5 and 6.6). Overall, rate-limited sorption and nonlinear sorption are uncertainties in evaluating the validity of the linear equilibrium sorption adopted in unsaturated zone transport studies. Rate-limited sorption reduces sorption in the matrix and increases the concentration and duration of migration through the fractures. In the TSPA-SR, the sorption coefficients (K_d s) of linear sorption for different radionuclides are represented by distribution functions to quantify the uncertainties (CRWMS M&O 2000a, Section 3.7.3).

Colloid Declogging—The kinetic declogging (reverse) coefficient, κ^- , is treated as a fraction of κ^+ to examine the sensitivity of this parameter on colloidal transport (CRWMS M&O 2000c, Figure 3.11-7). When no declogging is allowed, no colloids reach the water table (CRWMS M&O 2000ea, Section 6.16). Small values of κ^- (i.e., slow declogging) lead to retardation of colloids and slow transport to the water table. Large values of κ^- (i.e., fast declogging) lead to fast transport to the water table for radioactive colloids. For the TSPA-SR, the colloid retardation factor is conservatively set to 1 for all colloids in the unsaturated zone.

Surface Diffusion—It is possible that surface diffusion can be supported in zeolites. Surface diffusion can be important for radionuclides that exhibit strong sorption (e.g., plutonium). A larger K_d clearly indicates stronger sorption, but this does not mean immobilization of the dissolved species when the fractured porous medium supports surface diffusion (Moridis 1999, Section 6.1.2). For the TSPA-SR, the uncertainties of molecular diffusion coefficients (as described in Section 4.2.8.2.2, based on sorbing tritium and nonsorbing technetium measurements) and the retardation factors are independently sampled. The uncertainties associated with surface diffusion may be large for media supporting surface diffusion.

Desorption from Radioactive Decay—Daughters of sorbed parents may be ejected from grain surfaces because of recoil from radioactive decay. The alpha decay is evaluated and the potential implications for kinetically controlled sorption are discussed in *Radionuclide Transport Models under Ambient Conditions* (CRWMS M&O 2000ea,

Section 6.2.8). For equilibrium sorption, this is not an issue.

Particle Tracking—Different approaches to represent matrix diffusion could yield different transport behavior. Comparisons between the FEHM V2.10 particle tracker and DCPT code were performed by *Analysis Comparing Advective–Dispersive Transport Solution to Particle Tracking* (CRWMS M&O 2000ee, Section 6.4). The two particle-tracking routines agree only if diffusion and dispersion are neglected. For the cases that include diffusion and dispersion, the median breakthrough for FEHM V2.10 occurs at times more than one or two orders of magnitude earlier. The difference is more pronounced for radionuclides undergoing sorption in the matrix. These differences stem from different implementations of the diffusive mass flow between fractures and the matrix in the two codes (CRWMS M&O 2000ee, Section 7). The conservative FEHM V2.10 particle tracker is used for the TSPA-SR abstraction. The flow fields derived from the three-dimensional site-scale model are inputs to the particle tracker and are used to calculate transport velocities.

4.2.8.4 Total System Performance Assessment Abstraction

Unsaturated zone transport is important as the first natural barrier to radionuclides that escape from the potential repository. The unsaturated zone acts as a barrier by delaying radionuclide movement. If the transport time is long compared to the radionuclide half-life, then the unsaturated zone may have an important effect on decreasing the dose from that radionuclide at the biosphere. In this section, the abstraction of unsaturated zone process modeling results into the TSPA-SR is presented (CRWMS M&O 2000a, Section 3.7).

Within the unsaturated zone, radionuclides can migrate in groundwater as dissolved molecular species or associated with colloids (CRWMS M&O 2000a, Section 3.7.1). Five basic processes affect the movement of dissolved or colloidal radionuclides: advection, diffusion, sorption, hydrodynamic dispersion, and radioactive decay. Sorption is potentially important because it slows, or retards, the transport of radionuclides. Diffusion

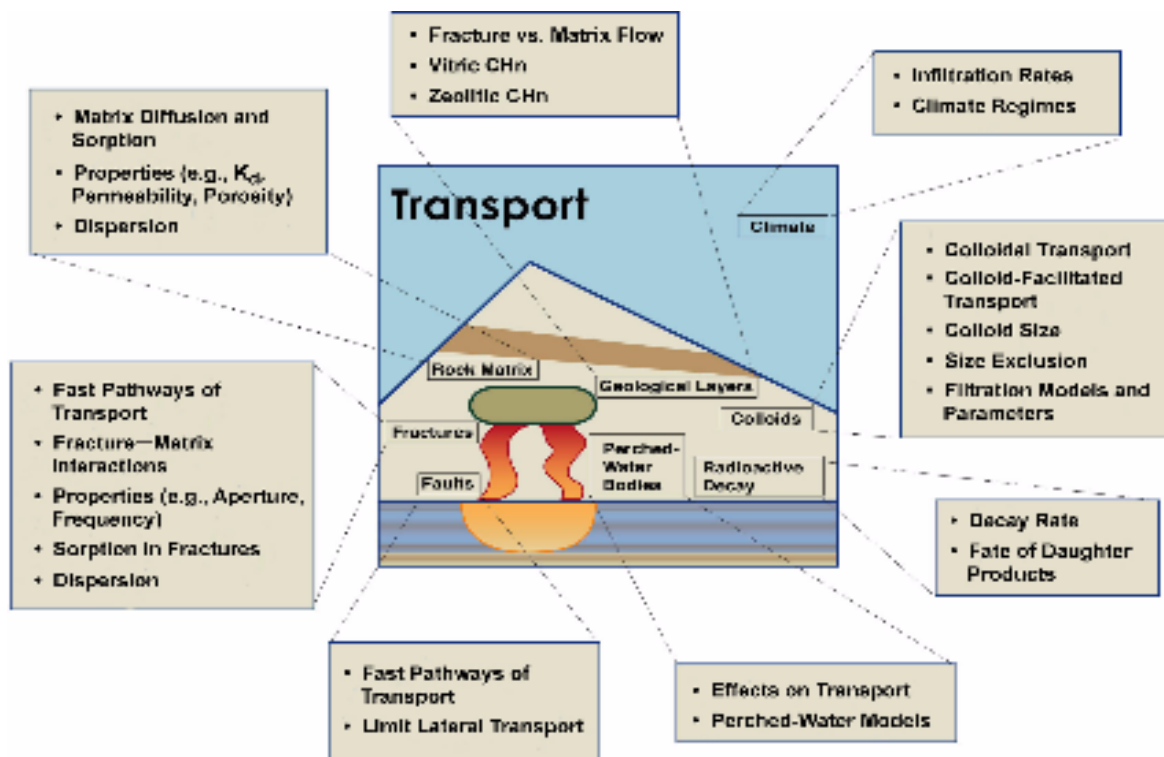
of radionuclides out of fractures into matrix pores is also a potential retardation mechanism because matrix transport is generally slower than fracture transport. However, sorption and matrix diffusion have less effect on colloids, so radionuclides can be more mobile if they are attached to colloids than if they are dissolved in the water. Radioactive decay is potentially important because daughter products may have sorption behavior different than that of the parent radionuclide, thus affecting transport. The key processes and issues for unsaturated zone transport are summarized in Figure 4-126. The unsaturated zone flow and transport model is used to represent the key processes, assess the uncertainties, and provide direct inputs to the TSPA-SR.

4.2.8.4.1 Abstraction and Direct Use of the Unsaturated Zone Flow and Transport Fields

A dual-permeability model is used to represent mountain-scale unsaturated zone flow. The same concept is used to model radionuclide transport: a dual-continuum model in which fractures and matrix are distinct interacting continua that coexist at every point in the modeling domain. Each continuum is assigned transport properties in addition to its hydrologic properties. The properties can vary spatially.

The unsaturated zone transport model is directly coupled, that is, dynamically linked, with the TSPA-SR model (CRWMS M&O 2000a, Section 3.7.2). The unsaturated zone flow calculations are done ahead of time, and the flow fields are saved for use by the TSPA-SR model. During a TSPA simulation, radionuclide mobilization and transport through the engineered barrier system are calculated and the radionuclide mass flux at the engineered barrier system boundary at each time step is provided as the boundary condition for unsaturated zone transport.

The use of pregenerated flow fields implies the assumption of quasi-steady flow. That is, flow is modeled as a sequence of steady states (as an approximation). Mountain-scale unsaturated zone flow is represented as a sequence of steady states as determined by climate change and infiltration models. The transport calculation (particle



002500-APP-21042-1000a

Figure 4-126. Key Issues of Unsaturated Zone Transport
Source: CRWMS M&O 2000c, Figure 3.11-1.

tracking) itself is fully transient, with radionuclides moving downward from the potential repository as they are released. Each TSPA realization uses one set of flow fields: low infiltration, mean infiltration, or high infiltration; each set has three flow fields, for present-day, monsoon, and glacial-transition climates.

The flow field is changed from one to another at the time of a climate change. The transport calculation then continues with the new flow field. In addition to the step change in the flow field, the location of the water table is also changed at the time of climate change. The water table for the future climates (monsoon and glacial-transition) is taken conservatively to be 120 m (390 ft) higher than the present-day water table (CRWMS M&O 2000ca, Section 6.2). When the water table rises with a climate change, radionuclides in the unsaturated zone between the previous and new water table elevations are moved to the saturated zone.

4.2.8.4.2 Abstraction of Matrix Diffusion, Sorption, and Dispersion

The incorporation of matrix diffusion in the unsaturated zone transport model is simplified by conservatively neglecting flow in the matrix continuum in the diffusion calculation. This allows use of an analytical solution for matrix diffusion (CRWMS M&O 2000ed, Section 6.1.3). Fracture properties (aperture, spacing) are modified to take into account that only some fractures actively flow and transport radionuclides (CRWMS M&O 2000ed, Section 6.2.1). Colloids are larger than solute molecules, so they have much smaller diffusion coefficients. Because of this and possible size-exclusion effects, matrix diffusion is conservatively neglected for colloids. Anionic species such as pertechnetate (the predominant aqueous species of technetium) have lower diffusion coefficients than cationic species (CRWMS M&O 2000c, Section 3.11.3.2) and are assigned different diffusion coefficients.

In TSPA simulations, the sorption characteristics of the tuff units are taken to be constant in time. Changes in sorption (or other transport properties) brought about by thermal effects of the potential repository or from climate change have been considered and found to be insignificant (CRWMS M&O 2000ef, Sections 6.3.8 and 6.8).

In unsaturated zone TSPA transport calculations, dispersion in fractures is represented independently of that in the matrix (CRWMS M&O 2000a, Section 3.7.1.4). Dispersion is a way of including small-scale velocity variations in the transport model, but these small-scale variations are not very important to unsaturated zone transport because they have less effect over long distances than the large-scale velocity variations that are explicitly included in the model. Also, the explicitly modeled differences in transport velocity between fractures and matrix, and the transfer of radionuclides between them, introduce considerable dispersion into the transport simulations. Transverse dispersivities are normally small compared to longitudinal dispersivities (CRWMS M&O 2000a, Section 3.7.1.4). Any transverse dispersion (spreading) that occurs in the unsaturated zone is eliminated at the water table by starting the saturated zone transport model at a small number of discrete points.

4.2.8.4.3 Abstraction of Colloidal Transport

Colloids diffuse more slowly than dissolved radionuclides because of their larger size, and as a result, matrix diffusion of colloids is neglected in TSPA. Colloids can, however, move between fractures and rock matrix advectively (i.e., moving with the water) as long as they are smaller than the matrix pores. Most of the pores in the welded and zeolitic tuffs are small, so most colloids remain in the fractures in those hydrogeologic units (CRWMS M&O 2000c, Section 3.11.3.4). Because transport in fractures is faster than transport in the matrix, this size-exclusion effect results in faster colloidal transport in those units. Most flow and transport in those units is through fractures, so the result of this effect is not large. In addition, a size-exclusion effect is possible at hydrogeologic unit interfaces. This exclusion is not applied to colloids transporting through fractures because fractures are

relatively large compared to matrix pores, but it is applied to colloids transported in the matrix from one hydrogeologic unit to another. In this situation a portion of the colloids, corresponding to the fraction of them that are smaller than the pores in the downstream unit, is stopped at the unit interface. This exclusion is taken to be a permanent filtration for irreversible colloids; it is not applied to reversible colloids because the radionuclides can desorb from the colloids and continue to move (CRWMS M&O 2000c, Section 3.11.13.3).

Colloids may be temporarily “detained” at the interface of fractures and matrix or sorbed to fracture walls (reversible filtration), and this interaction can be included in the colloid transport model as a retardation factor for colloid transport in the fracture system (CRWMS M&O 2000c, Section 3.11.13.3; CRWMS M&O 2000ed, Section 5.3). The effective transport velocity is reduced by this retardation factor. However, the data available on this effect are for the saturated zone, so the retardation factor is conservatively set to 1 in the unsaturated zone (i.e., no retardation due to this factor).

For reversible colloids, radionuclides sorbed to colloids are assumed to be in equilibrium with radionuclides in solution. The ratio of the concentration of a radionuclide sorbed to colloids to the concentration in solution is represented by a colloid partitioning factor in the models (CRWMS M&O 2000ed, Section 5.3). The ratio is a function of the concentration of colloids and the sorption coefficient for the given radionuclide onto the given type of colloid. Diffusion of dissolved radionuclides into the matrix can reduce the concentration in the fractures, which reduces the amount of radionuclides sorbed to the colloids in equilibrium with radionuclides in solution. Thus, matrix diffusion can effectively slow the transport. The colloid partitioning factor is one of the key transport parameters sampled in the TSPA-SR (CRWMS M&O 2000a, Section 3.7.3).

4.2.8.4.4 Abstraction with Particle Tracking

Radionuclide transport modeling for the unsaturated zone uses the residence time transfer function particle-tracking technique (CRWMS M&O

2000c, Section 3.11.13.3). This technique is a cell-based approach in which particles move from cell to cell in a numerical grid. Particle locations within cells are not tracked as they are in some particle-tracking techniques, but rather movement from cell to cell is computed probabilistically based on transfer functions. The transfer functions are defined using analytical or semi-analytical solutions of the transport equations and represent probability distributions of the residence time (the amount of time that a particle resides in a cell). The probability that a particle will move to a neighboring cell is proportional to the water flow rate to that cell. Only outflows are included in this calculation; particles are not moved to a cell if water flows from that cell to the current cell. A dual-continuum conceptual model is used for transport, so there is a network of fracture cells and a network of matrix cells, with each fracture cell connected to a corresponding matrix cell.

4.2.8.4.5 Abstraction of Spatial and Temporal Variabilities

Releases from the engineered barrier system are computed for 30 environmental groups that are based on infiltration, waste type, and seepage condition (CRWMS M&O 2000a, Section 3.7.2). Because infiltration is important for unsaturated zone transport, radionuclides are released into the unsaturated zone at locations consistent with the environmental group from which they are released. Each environmental group is associated with one of five infiltration categories that are based on the percolation at each spatial location during the glacial-transition climate. The ranges for the categories are 0 to 3 mm/yr (0 to 0.1 in./yr), 3 to 10 mm/yr (0.1 to 0.4 in./yr), 10 to 20 mm/yr (0.4 to 0.8 in./yr), 20 to 60 mm/yr (0.8 to 2.4 in./yr), and greater than 60 mm/yr (2.4 in./yr).

To avoid artificial dispersion, the model of radionuclide release into the unsaturated zone takes into account the number of failed waste packages within each of the five infiltration categories (CRWMS M&O 2000a, Section 3.7.2). If only one waste package has failed in a category, then releases for that category are put into a single unsaturated zone cell, sampled randomly from the cells in that category. If two waste packages fail,

then releases are put into two randomly selected cells. This process continues for additional waste packages until the number of failed waste packages is equal to the number of cells in the category; at that point the releases are spread over all cells in the category, and additional waste package failures cause no change in the release locations. For any number of failed waste packages in a particular category, releases are always divided evenly among the cells that have been selected. Artificial dispersion in the unsaturated zone is further reduced by gathering releases from the unsaturated zone into a few discrete locations at the water table for input to the saturated zone transport model.

In the unsaturated zone transport model, spatial variability is included by use of a three-dimensional model that incorporates the appropriate geometry and geology (CRWMS M&O 2000a, Section 3.7.3). Temporal variability is included by using different unsaturated zone flow fields for different climate states, but none of the other transport properties change with time.

4.2.8.4.6 Uncertainty and Conservatism

Uncertainty is included in the unsaturated zone transport model by defining uncertainty distributions for a number of input parameters. Values of these parameters for each TSPA realization are sampled from the distributions. Thus, each realization of the total system has a unique set of input parameters, each of which is within the range that is considered to be defensible (CRWMS M&O 2000a, Section 3.7.3). Normally each realization is considered to be equally likely, but importance sampling may be used to emphasize some realizations (usually to increase the probability of sampling an unlikely parameter value).

Current performance assessment models of unsaturated zone transport consider and account for uncertainties and conservatisms. These are detailed in *Unsaturated Zone Flow and Transport Model Process Model Report* (CRWMS M&O 2000c); they include:

- The significance of fracture flow in the vitric Calico Hills nonwelded hydrogeologic unit

- The effectiveness of perched water to divert water away from the zeolitic Calico Hills nonwelded hydrogeologic unit
- The reduction of fracture–matrix interaction along fractured flow paths within the Topopah Spring welded hydrogeologic unit
- The extrapolation of properties for the fault intervals in the Calico Hills nonwelded hydrogeologic unit and the Crater Flat undifferentiated hydrologic unit from fault data collected in the Topopah Spring welded hydrogeologic unit
- The use of a conservative particle tracker for performance assessment.

This conservatism may be partially offset by the use of batch-derived retardation factors (obtained from crushed-rock samples) for radionuclide migration, which may overestimate sorption (CRWMS M&O 2000c, Section 3.11.10.2). In general, the abstraction represents a balance of conservative assumptions and nominal parameters and processes to yield a reasonably realistic representation and assessment.

As noted in Section 4.1.1.2, the DOE has completed several activities to improve the treatment of uncertainty in current models, and the results are reported in *FY01 Supplemental Science and Performance Analyses* (BSC 2001a; BSC 2001b). Modeling based on new information and one-off sensitivity studies were focused on model aspects that were identified as unevaluated or that were perceived as having overly conservative estimates of uncertainty associated with them (BSC 2001b, Table 1.3-1). Descriptions of each analysis are contained in Volume 1 of *FY01 Supplemental Science and Performance Analyses* (BSC 2001a) and an assessment of the impact of the analyses on performance is presented in Volume 2 (BSC 2001b). In addition, analyses and assessments were carried out that provide a basis for evaluation of the role of repository thermal operating mode on performance and uncertainty. Analyses of performance of thermal modes are presented in Volume 2, Section 4 of *FY01 Supplemental Science and*

Performance Analyses (BSC 2001b). The supplemental analyses indicate that the TSPA-SR model is generally conservative to reasonable. The sensitivity studies are also briefly described in Section 4.4.5.5.

4.2.9 Saturated Zone Flow and Transport

Yucca Mountain is part of the Alkali Flat–Furnace Creek subbasin of the Death Valley flow system. Recharge within the Death Valley flow system occurs at high altitudes, where relatively large amounts of snow and rainfall occur. Water inputs to the Alkali Flat–Furnace Creek subbasin include groundwater inflow along the northern boundary of the subbasin, recharge from precipitation in high-elevation areas of the subbasin, and recharge from surface runoff in Fortymile Canyon and Fortymile Wash. North and northeast of Yucca Mountain, recharge from precipitation is believed to occur also at Timber Mountain, Pahute Mesa, Rainier Mesa, and Shoshone Mountain (CRWMS M&O 2000bn, Section 3.2).

The geologic strata at Yucca Mountain form a series of alternating volcanic aquifers and confining units above the regional carbonate aquifer. The volcanic rocks generally thin toward the south, away from their eruptive sources in the vicinity of Timber Mountain. The volcanic aquifers and confining units are intercalated with undifferentiated valley-fill and the valley-fill aquifer to the south and southeast of Yucca Mountain (USGS 2000d, Section 6.1).

The general conceptual model of saturated zone flow in the site-scale saturated zone flow and transport model area is that groundwater flows to the south from recharge areas of higher precipitation at higher elevations north of Yucca Mountain, through the Tertiary volcanic rocks into the valley-fill aquifer, and toward the Amargosa Desert. Within the site-scale model area, recharge occurs from infiltration of precipitation and infiltration of flood flows from Fortymile Wash and its tributaries. Outflow from the model area mostly occurs across the southern boundary of the model, and to pumpage by irrigation wells in the Amargosa Farms area (CRWMS M&O 2000bn, Section 3.2).

In the event of waste mobilization and migration away from the potential emplacement drifts at Yucca Mountain, the rate of radionuclide transport through the saturated zone is determined by the groundwater flux, the hydrologic properties, and sorptive properties of tuff and alluvium units.

The objective of the saturated zone flow and transport process model and the corresponding components of the TSPA-SR is to evaluate the migration of radionuclides from their introduction at the water table below the potential repository to

the release point to the biosphere, as illustrated in Figures 4-127 and 4-128. The release point is at the accessible environment downgradient (i.e., the direction of groundwater flow) from the site. The main output of the saturated zone flow and transport process models used directly by the TSPA is an assessment of the concentration of radionuclides in groundwater and the time it takes for various radionuclides to be transported from areas beneath the potential repository to the accessible environment. The current understanding of saturated zone transport is documented in *Saturated Zone Flow*

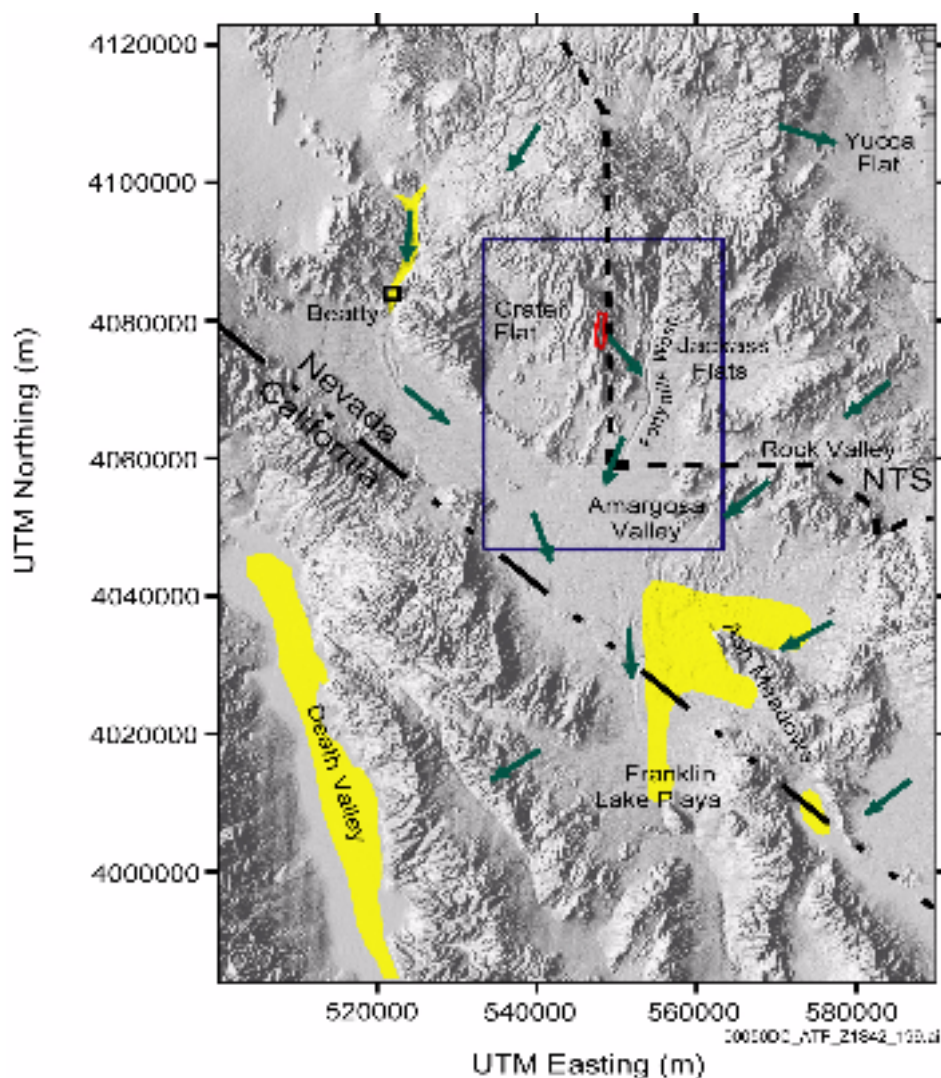


Figure 4-127. Regional Map of the Saturated Zone Flow System Showing Direction of Flow and Outline of the Three Dimensional Saturated Zone Flow Model Domain

Arrows give direction of flow from regional flow models. The solid rectangle shows the boundary of the site-scale three-dimensional saturated zone flow model. Flow from Yucca Mountain is southeast to Fortymile Wash and then south to the site-scale model boundary. NTS = Nevada Test Site. Source: (CRWMS M&O 2000a, Figure 3.8-4).

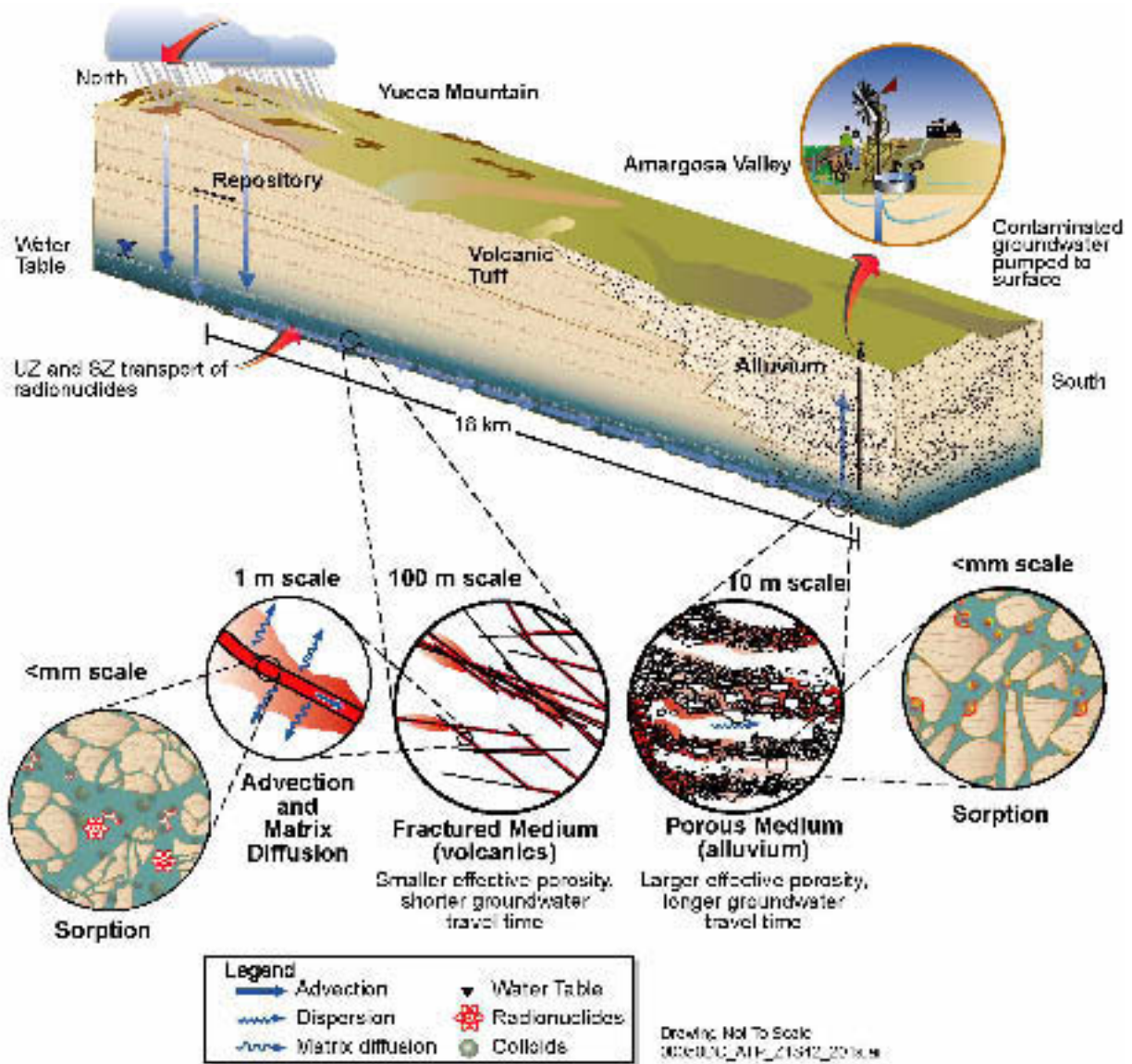


Figure 4-128. Conceptualization of Features and Processes Important to Saturated Zone Transport

This schematic illustration presents transport processes in fractured and porous media flow at Yucca Mountain, providing a conceptualization of transport through the saturated zone to the location of the reasonably maximally exposed individual in the Amargosa Valley. Moving groundwater carries (advects) dissolved or suspended radionuclides in fractures in the volcanic rocks and in pores between individual rock grains in the alluvium. The processes of diffusion and sorption slow the transport of radionuclides to the accessible environment. Radionuclides diffuse into and out of the unfractured portion (matrix) of the volcanic rocks. In the alluvium, radionuclides diffuse into and out of regions where water is stagnant or flows very slowly. UZ = unsaturated zone; SZ = saturated zone.

and Transport Process Model Report (CRWMS M&O 2000bn).

4.2.9.1 Conceptual Basis of Flow and Transport

The following discussion of the conceptual basis for the site-scale saturated zone flow and transport model is a summary of information presented in Section 3.2 of *Saturated Zone Flow and Transport Process Model Report* (CRWMS M&O 2000bn).

Flowing groundwater transports radionuclides either in solution (dissolved) or in suspension, bound to very small particles known as colloids. Colloid particles are small enough to travel with flowing water through fractures in volcanic rocks, pores in the unfractured portion (matrix) of volcanic rocks, and pores in alluvium. Radionuclide releases from water contacting breached waste packages in the potential repository would have to migrate a distance ranging from approximately 210 m (690 ft) to 390 m (1,300 ft) downward to the water table, then migrate down-gradient in the saturated zone to reach the accessible environment. The average distance of the potential repository above the elevation of the water table is about 300 m (1,000 ft). Groundwater in the saturated zone generally moves southeast from beneath the potential repository before flowing south out of the volcanic rocks and into the thick valley fill deposits of the Amargosa Desert.

The water table under most of the potential repository is in the Tertiary age Crater Flat Group. This stratigraphic unit is also referred to by a hydrostratigraphic name, the lower volcanic aquifer. It is composed of three tuffs: the Tram, Bullfrog, and Prow Pass. After reaching the water table, flow continues away from the immediate vicinity of the potential repository site in the Crater Flat Group. Permeability of tuffs in the Crater Flat Group is small where the rocks are not fractured. Consequently, most flow of groundwater in these rocks occurs in fractures.

The volcanic rocks are about 2,000 m (6,500 ft) thick at the site, but they gradually thin to 0 m (0 ft) with increasing distance from the site. At a distance of 10 to 20 km (6 to 12 mi) along the

travel path from the potential repository, groundwater flow enters alluvium and remains in alluvium to the accessible environment. Flow in alluvium is modeled as movement through pores between rock grains rather than in fractures.

The quantity of groundwater that flows through a unit area of rock per unit period of time is known as the specific discharge. To maintain the same specific discharge in volcanic rocks and alluvium, the velocity of flow must be slower in the alluvium because the effective porosity of the alluvium is larger than the fracture porosity of the volcanic rocks. Results of the saturated zone site-scale flow model show that specific discharge does not change greatly along flow paths from the repository to the receptor location. Consequently, flow velocities are faster in volcanic rocks than in alluvium. Figure 4-129 shows possible flow paths from the potential repository, as well as the portions of the flow paths in tuff and alluvium. The portion of the flow paths in tuff is shown in red, and the portion in alluvium is blue. The location of the contact of tuff and alluvium is uncertain and is treated stochastically in TSPA-SR calculations. This figure shows the contact to be at the expected-value location.

The flow paths described previously are inferred from a site-scale flow model. This model results in a flow field that is consistent with available information concerning geology, rock hydraulic properties, groundwater chemistry, and measured water levels. One feature of the simulated three-dimensional flow field is higher hydraulic head in carbonate rocks at depth than in the rocks containing the simulated flow paths from below the potential repository. The carbonate rocks are relatively permeable and laterally continuous. They are sometimes referred to by the hydrostratigraphic name, the regional carbonate aquifer. The upward gradient of hydraulic head from the carbonate rocks to the overlying tuffs is observed in boreholes located within the more extensive Death Valley Regional Flow System and is supported by regional-scale flow modeling (D'Agnese, Faunt et al. 1997). In addition, the upward gradient is observed in the only borehole in the vicinity of Yucca Mountain to penetrate the regional carbonate aquifer. This potential for upward flow is

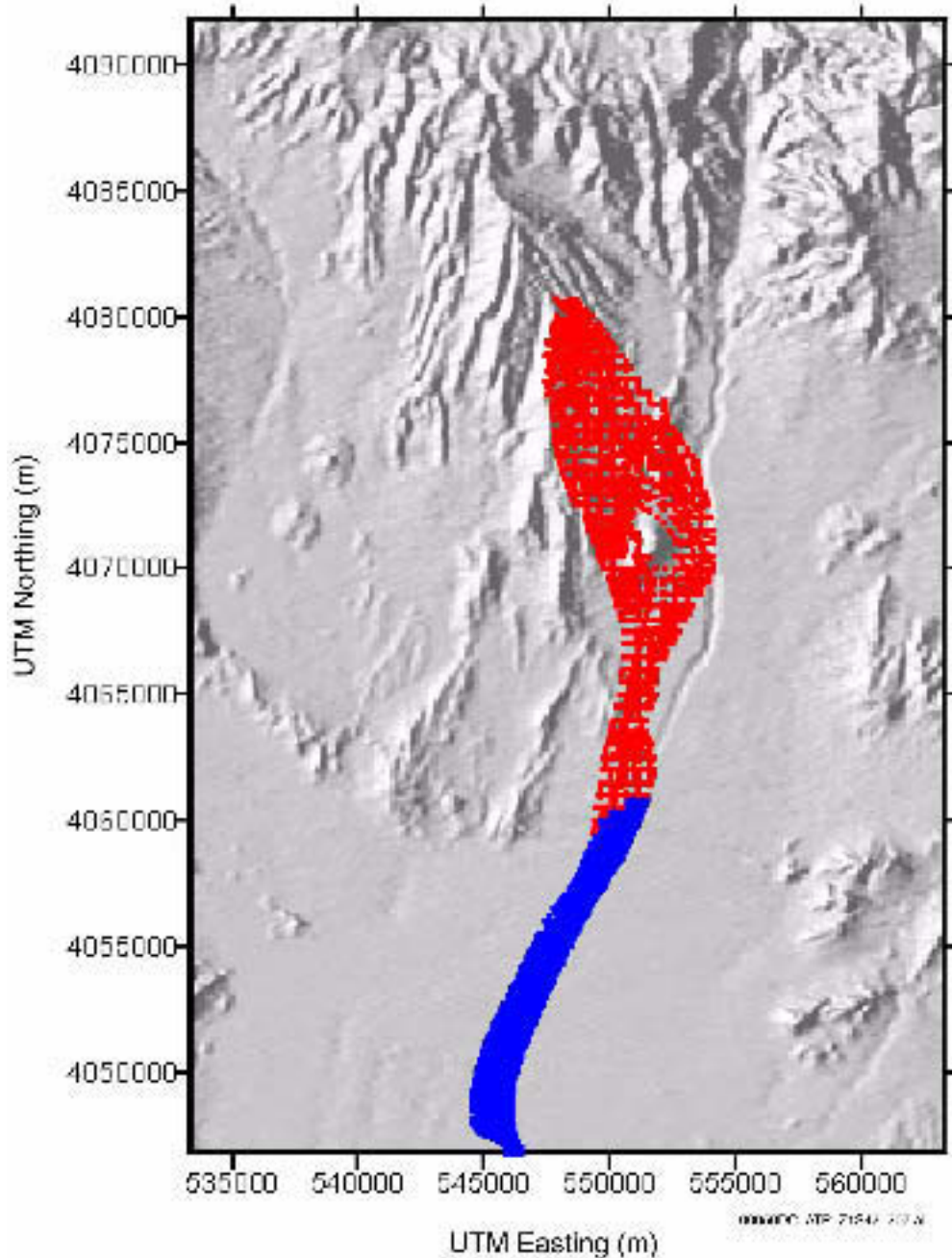


Figure 4-129. Flow Paths Predicted by the Site-Scale Saturated Zone Flow and Transport Model for the TSPA-SR

The repository is located in the upper central part of the figure. The released particles move from the upper central area in the figure to the bottom. The red portion of the illustrated particle positions corresponds to an area of flow through fractured volcanic tuff while the blue part of the flow path is through alluvium, modeled as a porous medium. The spatial pattern in the volcanic tuff reflects the numerical algorithm that illustrates particle positions at grid boundaries or at the end of a time step. The location of the contact of tuff and alluvium is uncertain and is treated stochastically in TSPA-SR calculations. This figure shows the contact to be at the expected-value location. Source: Adapted from CRWMS M&O 2000a, Figure 3.8-21.

significant for the performance of the potential repository because it prevents downward flow of contaminants from Yucca Mountain into the regional carbonate aquifer.

Several processes act to slow the movement of radionuclides or to dilute their concentration (Figure 4-128). The processes that slow, or retard, the movement of radionuclides are important in that longer travel times allow more time for radioactive decay to occur. One important retardation process is sorption onto mineral surfaces. The sorption process is reversible. Consequently, a portion of the radionuclides at a particular location will be sorbed to rock surfaces, and a portion will be in solution in the groundwater. Multiple cycles of sorption and desorption slow the movement of radionuclides relative to the groundwater flow rate.

Diffusion of dissolved or colloidal radionuclides into regions of very slowly moving groundwater is a second important retardation process. Diffusion will occur from water flowing in the fractures of the volcanic rocks into the matrix, or nonfractured, portion of these rocks, as well as from water in pores between rock grains in the alluvium into porosity within the rock grains. In either case, the radionuclides will eventually diffuse back out into the moving groundwater. However, multiple cycles of diffusion into and out of the rock matrix and grains slows the rate of transport.

Finally, hydrodynamic dispersion, or spreading of solutes, along the flow path can decrease the concentration of radionuclides in groundwater (Figure 4-130). Dispersion is mainly due to differences in flow velocity at a microscopic scale or by larger-scale heterogeneity of permeability.

4.2.9.2 Summary State of Knowledge

In this section, data are presented that support selected aspects of the conceptual basis and modeling of radionuclide transport through the saturated zone. In addition, natural analogues for these processes are discussed.

The transport of radionuclides potentially released from a repository is closely tied to the behavior of water flowing through the host subsurface material

because liquid water is the principal medium in which radionuclides are transported to the potential downgradient receptor (CRWMS M&O 2000bn, Section 3). If released, radionuclides would primarily move in groundwater as solute or attached to colloids. The transport of radionuclides as solute is affected by the three processes discussed in the previous section—advection, diffusion, and dispersion—and, for reactive constituents, by sorption. In addition, transport of radionuclides attached to colloids is affected by filtering, in which colloids with diameters greater than the pore openings are “sieved” by the medium. Transport of filtered particles is thereby retarded with respect to advective flow. Chemical precipitation, retardation (slowing the movement of radionuclides to less than the velocity of groundwater), and dilution (reducing the concentration) of radionuclides in the groundwater all affect the concentration of radionuclides released to the environment.

4.2.9.2.1 Advection

C-Wells Testing—Results from the hydraulic and tracer testing completed at the C-Wells Complex (Figure 4-131) were used to identify and confirm the conceptualization of flow and transport in the fractured tuff and to derive flow and transport parameters used in the modeling. Data from the testing are discussed in the next sections on advection, dispersion, matrix diffusion, and sorption. Ongoing testing at the Alluvial Testing Complex located at Nye County Well 19D, shown in Figure 4-131, will provide additional information on flow and transport in the alluvium.

Advection in the Fractured Porous Media—Hydrologic evidence supports the model of fluid flow within fractures in the moderately to densely welded tuffs of the saturated zone (CRWMS M&O 2000bn, Section 3.2.2). Bulk hydraulic conductivities measured in the field tend to be several orders of magnitude higher than hydraulic conductivities of intact tuff core samples measured in the laboratory. Also, there is a positive correlation between fractures identified using acoustic televiewer or borehole television tools and the zones of high transmissivity and flow (Erickson and Waddell 1985, Figure 3).

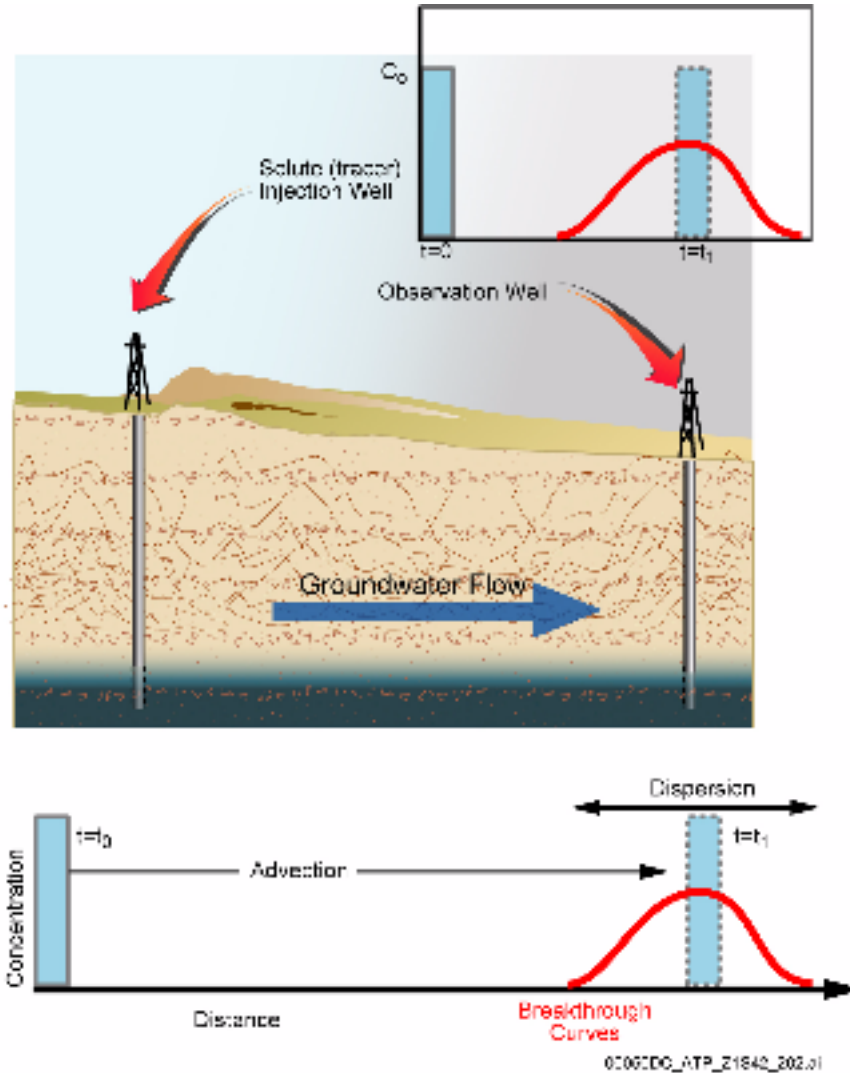


Figure 4-130. Concepts of Advection and Dispersion in Porous Medium and the Resulting Breakthrough Curves Defined by the Time History of Solute Concentration Measured in a Well

The initial volume at the well on the left illustrates the introduction of a solute plume at time $t=0$. As the solute moves downstream (by advection) to an observation well, it spreads by dispersion. The dotted volume illustrates the effect of advection only. The breakthrough curve gives the time-dependent concentration history at the observation well.

Fractures have important effects on the hydrology at Yucca Mountain, and the permeability distribution and principal flow directions depend strongly on the spatial distribution and orientations of fractures.

The laboratory work of Peters et al. (1984, Appendix E), in which fracture hydraulic apertures were found to be relatively insensitive to confining pressures, suggests that the spatial distribution of fractures (densities and interconnectivities) is more

important in determining hydraulic conductivity as a function of direction than the effect of the stress field on the apertures of individual joints.

Numerical simulations (Brown 1987) suggest that there is a propensity of fluid and solutes to travel preferentially along channels in fractures where apertures are largest. Thus, for flow within fractures in the saturated zone, a fracture-flow model recognizing and accounting for flow channels may be necessary.

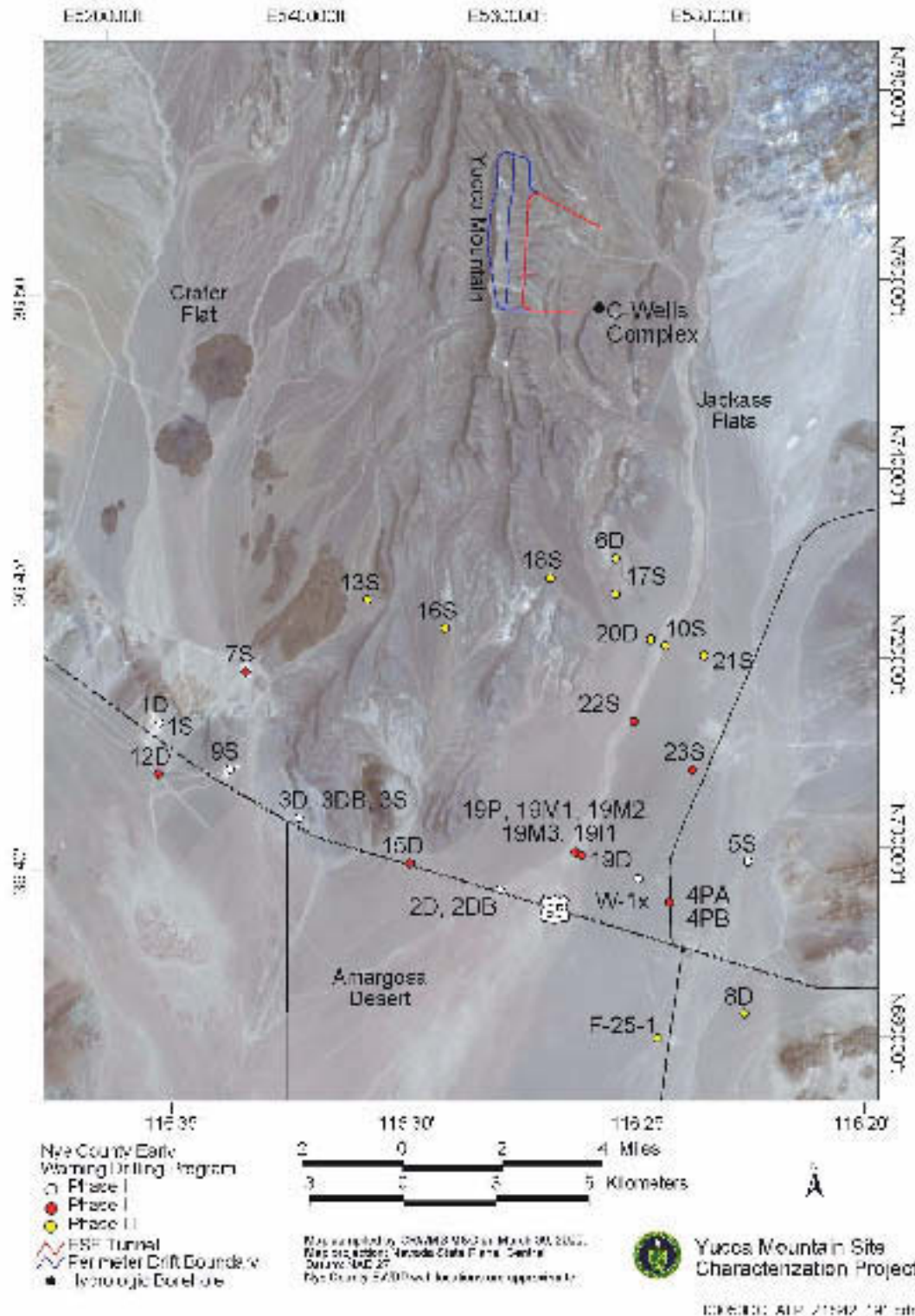


Figure 4-131. Nye County Early Warning Drilling Program Boreholes, the C-Wells Complex, and 19D (the Location of the Alluvial Testing Complex)
 Source: CRWMS M&O 2000bn, Figure 2-3.

Fractures generally are found within the moderately to densely welded tuffs, so the range of matrix porosities of these tuffs (0.06 to 0.09 for densely welded and 0.11 to 0.28 for moderately welded) probably best reflects the matrix fluid storage capacity of interest for saturated zone transport calculations (CRWMS M&O 2000bn, Section 3.2.4.1.1).

Advection in the Alluvium—Due to the more porous and less fractured nature of the porous alluvial material, fluid flow in the alluvium is well represented using a porous continuum conceptual model. However, this assumption does not mean that the medium is homogeneous. On the contrary, flow is likely to occur through the more permeable regions within the medium, with the low-permeability regions acting as flow barriers that groundwater flows around rather than through. Ongoing Nye County Early Warning Drilling Program drilling and the Alluvial Testing Complex

testing will provide more data to quantify the alluvium portion of the flow. Hydrologic parameters used in numerical models were selected to be conservatively bounding. Fluid flow is represented using a porous continuum with a constant and conservative permeability value. Transport parameters are assigned based on uncertainty distribution of the parameters.

Fracture Properties—Fracture properties (such as aperture, frequency, mineralogy, and saturation, as shown in Figure 4-132) affect fracture–matrix interactions, dispersion, sorption, and the transport of aqueous and colloidal species. The fracture apertures are derived from the fracture porosity and fracture–matrix connection area (CRWMS M&O 2000ed, Section 6.2.1). A log-normal distribution of apertures for all the model layers beneath the potential repository is sampled stochastically in the transport calculations for TSPA.

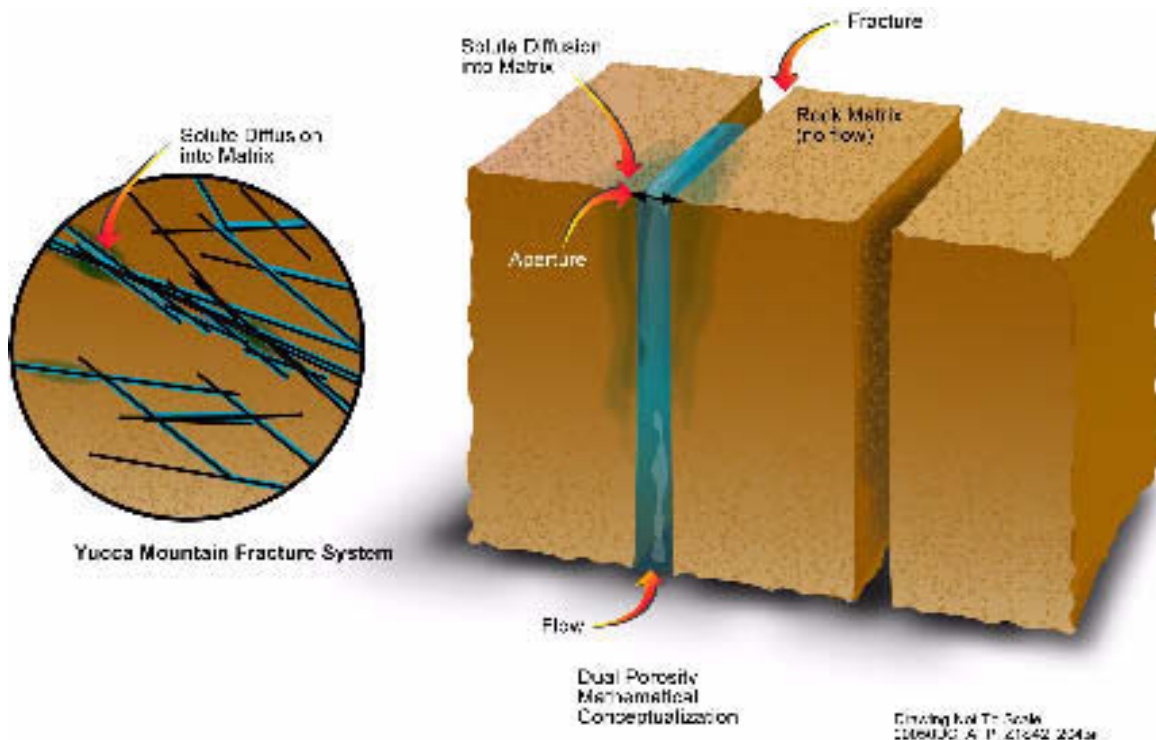


Figure 4-132. Fracture Properties of Aperture (Width), Length, and Frequency (Number of Fractures per Volume)

These parameters vary spatially in real geological media. The dual-porosity mathematical conceptualization assumes stagnant water in a porous rock matrix of high porosity and low permeability and relatively rapid flow in the fracture network of low porosity and high permeability. Solute enters and leaves the matrix rock through matrix diffusion.

In the saturated zone, the main distinction between the volcanic aquifers and the confining units is that the aquifers tend to be more welded and contain more permeable fractures. However, alteration of the tuffs to zeolites and clays, which reduces permeability, is more pronounced at depth, and the greater pressure at depth tends to reduce fracture permeability. Consequently, a combination of factors, including fracture properties, mineralogy, and depth, rather than just rock type, determines the hydrologic character of the volcanic rocks below the water table at Yucca Mountain.

Hydraulic tests have been performed to determine the properties of the saturated zone volcanic units. The analyses are limited by uncertainties about the extent to which fractures affect the unit conductivity (a measure of the ability of the subsurface material to transmit flow) (Luckey et al. 1996, pp. 32 to 36). However, the confining units had a low range of conductivities (0.000005 m to 0.26 m [0.00002 to 0.85 ft] per day), whereas the aquifers had a range of moderate to high conductivities (0.00004 m to 18 m [0.0001 to 59 ft] per day). Intervals without open fractures in all units tend to have low hydraulic conductivity, reflecting the conductivity of the rock matrix or of small fractures (Luckey et al. 1996, p. 32). Conversely, larger values of apparent hydraulic conductivity for both aquifers and confining units can generally be attributed to fractures.

Hydraulic tests at Yucca Mountain were performed in single-borehole and multiple-borehole tests (C-Wells Complex). Transmissivities, which are a measure of the ability of the entire thickness of the rock unit to transmit water, were measured in the multiwell tests and tend to be approximately 100 times greater than those determined from single-borehole tests in the same borehole. This observation suggests that the multiwell tests, which sample larger subsurface volumes, are also encountering a larger number of permeable fractures (Luckey et al. 1996, p. 36). The test results also support the hypothesis that fractures are more important than matrix in controlling hydraulic conductivity of the volcanic rocks in the saturated zone.

Groundwater Flow Paths—The concentrations of chemical constituents in groundwater that do not react with the subsurface material (i.e., conservative constituents) can be used to help delineate groundwater flow paths both on a regional and a local basis (CRWMS M&O 2000eg, Figure 5). Maps of areal variations in the concentrations of such constituents as chloride in the Yucca Mountain region delineate flow paths with generally north–south orientations (Figure 4-133). Flow paths from the potential repository first trend to the southeast towards Fortymile Wash and then, after reaching Fortymile Wash, trend more southerly. Whether water from the potential repository horizon mixes with water moving southward along Fortymile Wash is unclear. If such mixing does take place, it could substantially dilute the concentrations of any radionuclides that might be released from the potential repository. If not, radionuclides that might be released from the potential repository could be confined to the somewhat slower flow paths generating from below Yucca Mountain.

The time at which a given body of water is recharged can generally be bounded through an analysis of isotopic data for hydrogen, oxygen, carbon, and chlorine. Data on isotopic compositions of hydrogen and oxygen in saturated zone waters in the Yucca Mountain region suggest that the waters of southern Yucca Mountain and eastern Crater Flat infiltrated under cooler conditions than the waters of northern and eastern Yucca Mountain, which in turn were infiltrated under cooler conditions than waters along Fortymile Wash (CRWMS M&O 2000eg, Section 6.5.4.1). Through comparisons of the isotopic data for waters in modern climatic regimes, it is likely that the cooler conditions reflected in the waters of southern Yucca Mountain and eastern Crater Flat were associated with the end of the last ice age approximately 10,000 years ago. Carbon isotopic data (including carbon-14 measurements) for these waters are consistent with such a conclusion (CRWMS M&O 2000eg, Section 6.5.4.2.1). Unfortunately, the carbon isotopic data do not allow the derivation of more accurate groundwater ages because of uncertainty in the degree to which the original atmospheric carbon-14 signal in infiltrated waters may have been modified by dissolution of preexisting carbonate minerals. As a

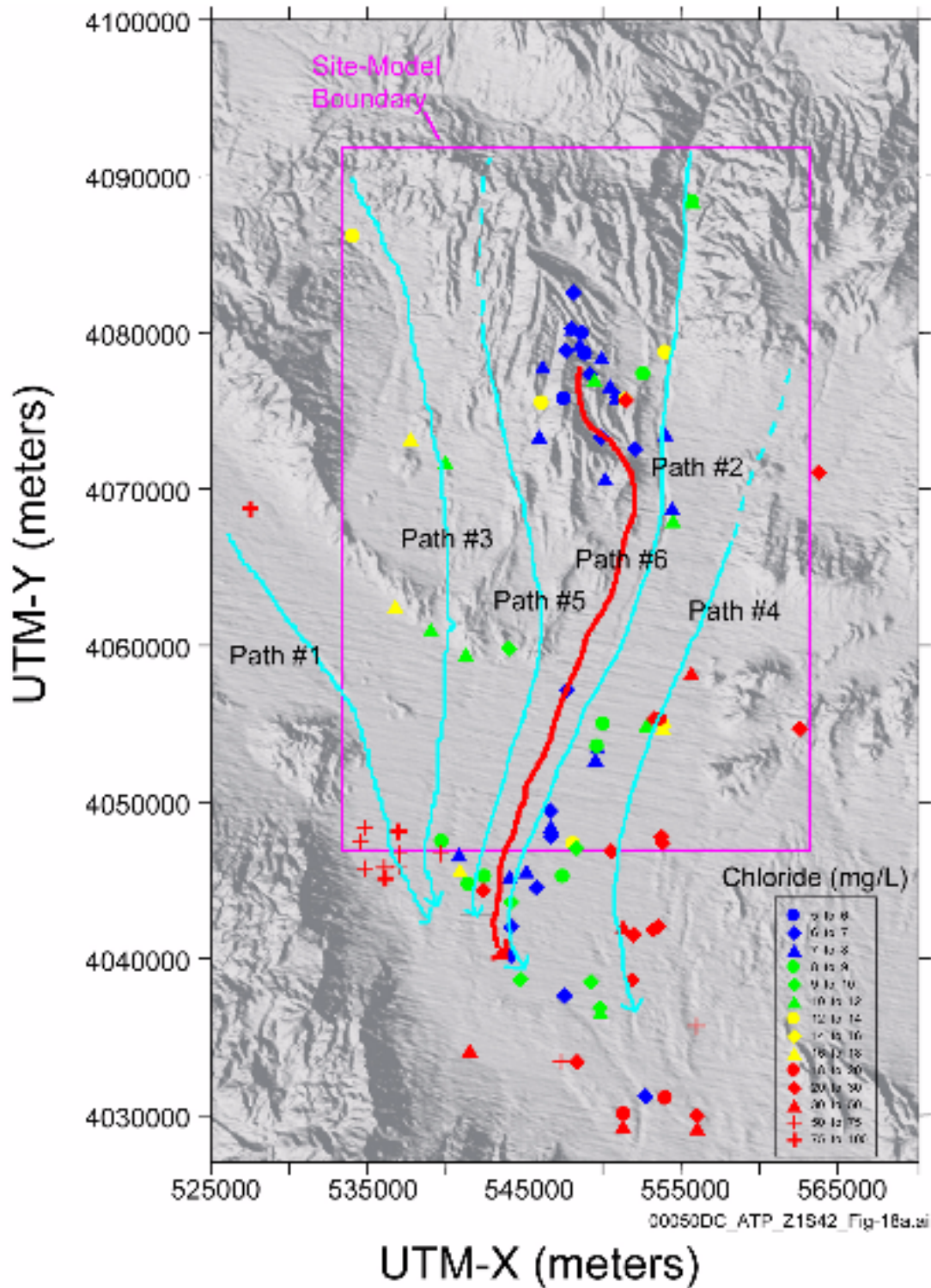


Figure 4-133. Groundwater Flow Paths near Yucca Mountain as Inferred from Chloride Concentrations at Sites near Yucca Mountain

The red arrow shows the groundwater flow path from Yucca Mountain. The blue arrows show other regional groundwater flow paths that constrain the Yucca Mountain flow path. UTM = Universal Transverse Mercator. Source: Modified from CRWMS M&O 2000bn, Figure 3-3.

consequence, groundwater ages calculated on the basis of observed carbon-14 values are maximum ages (CRWMS M&O 2000eg, Section 6.5.4.2.1).

The apparent age of groundwater in Fortymile Wash is younger than the age of groundwater beneath the potential repository (CRWMS M&O 2000eg, Section 6.5.4.2.1). This result implies that, if there is groundwater mixing, groundwater below the potential repository makes up at most a small fraction of the groundwater beneath Fortymile Wash. It also suggests the possibility that flow paths from the area of the potential repository may have a more southerly orientation than suggested by the chlorine data (Figure 4-133).

The expected flow path of groundwater moving away from the potential repository in the saturated zone passes into the valley-fill deposits approximately 15 km (9.3 mi) or more south of Yucca Mountain. Beginning in 1999, numerous boreholes have been drilled in the valley fill as part of the Nye County Early Warning Drilling Program (Figure 4-131). Additional holes are scheduled to be drilled in later phases. In addition to providing a monitoring system for Amargosa and Pahrump valleys, these holes are designed to provide information about the lithology, water levels, hydraulic properties, and transport properties of the valley fill. This information should enable the DOE to limit the uncertainties and conservatism in the current site-scale saturated zone flow and transport model.

4.2.9.2.2 Matrix Diffusion

Instead of simply traveling at the flow rate of the fluid in the saturated zone, radionuclides will potentially undergo physical and chemical interactions that must be characterized to predict large-scale transport behavior. In the laboratory, the effect of matrix diffusion has been clearly demonstrated by rock-beaker, diffusion-cell, and fractured-rock-column experiments (CRWMS M&O 2000eb, Section 6.6). Transport models incorporating matrix-diffusion concepts have been proposed to explain the inconsistencies between groundwater ages obtained from carbon-14 data and those predicted from flow data. In the field, interwell tracer tests that demonstrate the effect of

matrix diffusion have been conducted (CRWMS M&O 2000eb, Section 6). These laboratory experiments and field tests have demonstrated the validity of matrix diffusion and provided a basis for quantifying the effect of matrix diffusion on radionuclide migration through the moderately and densely welded tuffs of the saturated zone at Yucca Mountain. Because the effect of matrix diffusion on transport through the saturated zone could be important, it is incorporated into the TSPA model of radionuclide migration.

When a dissolved species travels with the groundwater within a fracture, it may migrate by molecular diffusion into the relatively stagnant fluid in the rock matrix. When a molecule enters the matrix, its velocity effectively goes to zero until Brownian motion carries it back into a fracture. The result of moving into the stagnant matrix is a delay in the arrival of the solute at a downgradient location from that predicted if the solute had remained in the fracture.

As described in *Saturated Zone Transport Methodology and Transport Component Integration* (CRWMS M&O 2000eh), mathematical models were first used to demonstrate the likely effect of matrix diffusion and flow in fractured media. In these studies, transport was idealized as plug flow in the fracture with diffusion into the surrounding rock matrix. Experiments were performed on transport in natural fissures in granite, and it was concluded that matrix diffusion was necessary to model conservative tracer data. The concept of matrix diffusion was extended to examine the coupling between matrix diffusion and channel flow usually thought to occur within natural fractures.

Often, groundwater ages obtained from carbon-14 data are greater than those predicted from flow data. Sudicky and Frind (1981) developed a model of flow in an aquifer with diffusion into a surrounding aquitard and showed that the movement of carbon-14 can be much slower than that predicted assuming only movement with the flowing water. Maloszewski and Zuber (1985) reached a similar conclusion with a model for carbon-14 transport that consists of uniform flow through a network of equally spaced fractures with

diffusion into the surrounding rock matrix. Their model also includes the effect of chemical-exchange reactions in the matrix, which further slows the migration velocity. They also present analyses of several interwell tracer experiments showing that the matrix-diffusion model can be used to provide simulations of these tests that are consistent with the values of matrix porosity obtained in the laboratory and aperture values estimated from hydraulic tests. In all cases, the results are superior to previous analyses that did not include the effects of matrix diffusion. Finally, of greatest relevance to the saturated zone beneath Yucca Mountain is the C-Wells reactive tracer test (CRWMS M&O 2000bn, Section 3.1.3.2), which demonstrated that models incorporating matrix

diffusion provide more reasonable fits to the tracer-experiment data than those that assume a single continuum. Maloszewski and Zuber (1985) demonstrated that a suite of tracers with different transport characteristics (diffusion coefficient, sorption coefficient) produced breakthrough curves that can be explained with a model that assumes diffusion of tracers into stagnant or near-stagnant water in the matrix pores (Figure 4-134).

Data from naturally occurring isotopes such as carbon-14 provide valuable clues into the processes controlling transport in the saturated zone. The apparent ages of saturated zone fluids are several thousand years or more (CRWMS M&O 2000bn, Section 3.1.2.3). These ages imply

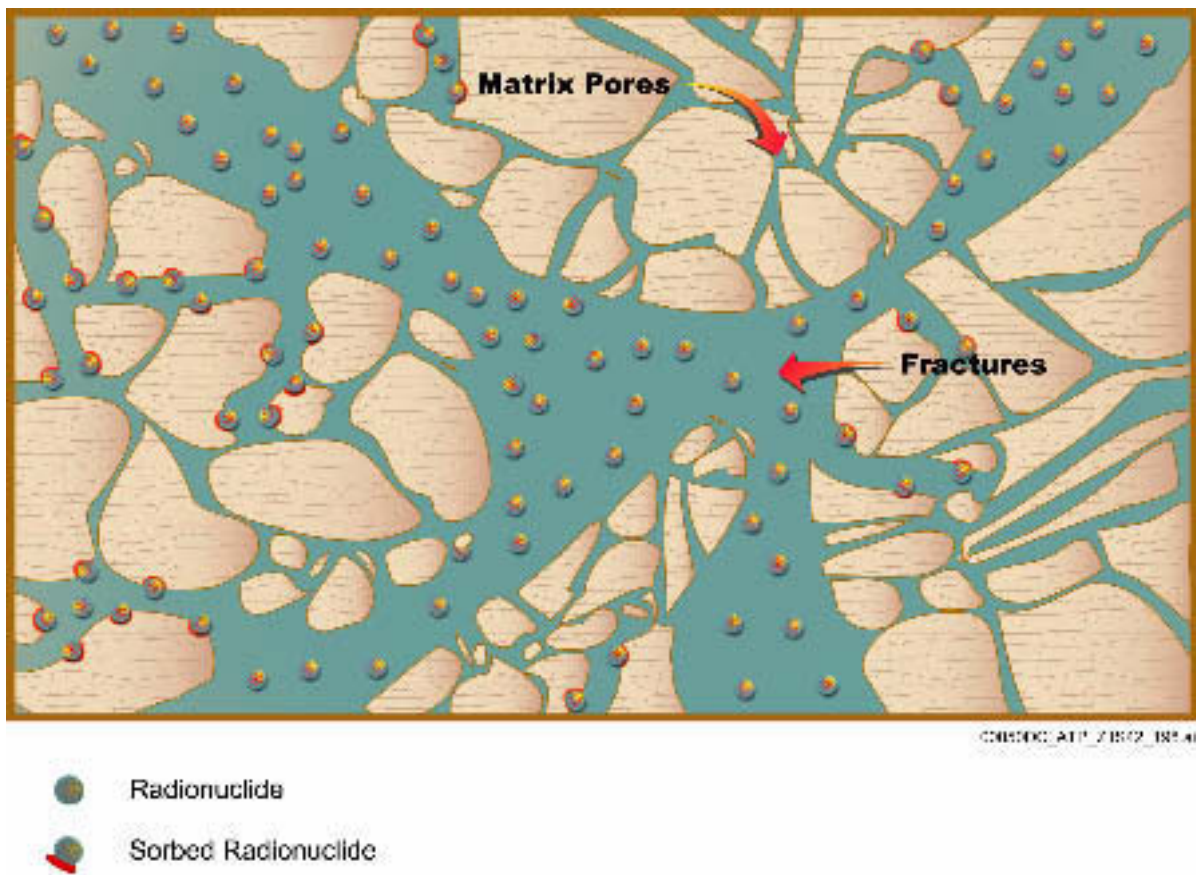


Figure 4-134. Conceptualization of Solute and Colloid Transport in a Fracture with Sorption in the Rock Matrix

Sorption in the fracture rock is conservatively ignored in TSPA-SR calculations. After diffusing into the matrix, solutes are sorbed into the rock matrix. Source: CRWMS M&O 2000a, Figure 3.7-4.

that either transport of carbon is slowed by matrix diffusion or advective porosity is much larger than expected for a fractured media. This argument is consistent with the conceptual model of interchange of solutes between the fractures and matrix found in the matrix-diffusion model (CRWMS M&O 2000bn, Section 3.2.4.2).

4.2.9.2.3 Hydrodynamic Dispersion

Dispersion is caused by heterogeneities from the scale of individual pore spaces to the thickness of individual strata and the length of structural features such as faults. The spreading and dilution of radionuclides that results for these heterogeneities could be important to performance of the potential repository. The largest heterogeneities are represented explicitly in the site-scale saturated zone flow and transport model (CRWMS M&O 2000bn, Section 3.2.4.4) in that these features are embodied in the hydrogeologic structure on which the model is built. For dispersion at smaller scales, dispersion is characterized using an anisotropic dispersion coefficient tensor consisting of a three-dimensional set of values: longitudinal, horizontal-transverse, and vertical-transverse dispersivities.

Transport field studies have been conducted at a variety of length scales from meters to kilometers to address the issue of dispersion, as discussed in *Saturated Zone Flow and Transport Process Model Report* (CRWMS M&O 2000bn, Section 3.2.4.4). Figure 4-135 shows estimated dispersivity as a function of length scale. The dispersivity values determined for the C-Wells reactive tracer experiment (CRWMS M&O 2000bn, Section 3.1.3.2), shown as a black diamond, illustrate a trend toward larger dispersion coefficients for transport over longer distances. Solutes encounter larger-scale heterogeneities at greater distances, and thus spreading is more pronounced. There is uncertainty in this estimate due to uncertainty in the exact flow paths taken by a tracer during the test. Nevertheless, the estimate falls within the range of values from other sites, suggesting that transport in the fractured tuffs exhibits similar dispersive characteristics. The values used in the simulations of radionuclide transport are somewhat higher than those estimated from the C-Wells because of the

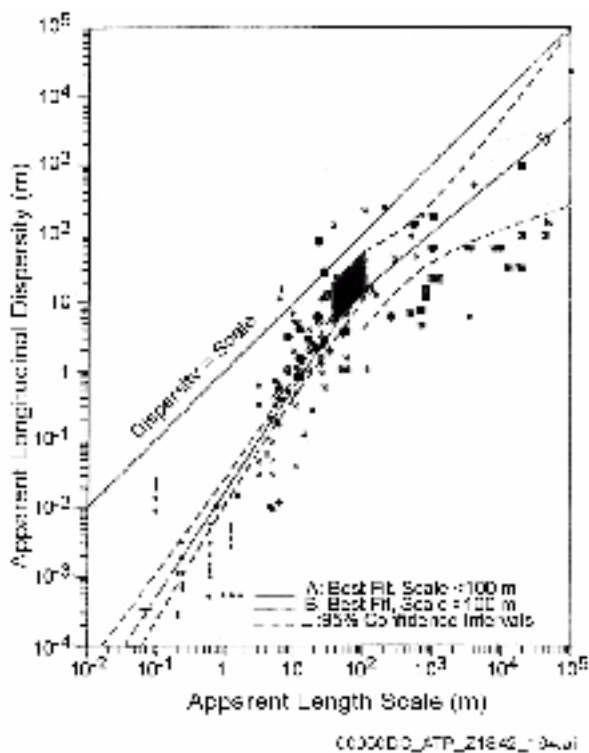


Figure 4-135. Estimated Dispersivity as a Function of Length Scale

The black diamond represents the dispersivity determined for the C-Wells reactive tracer experiment. Source: CRWMS M&O 2000eb, Figure 100.

larger scale that is relevant for radionuclide migration to the receptor location. A discussion of the numerical and field studies used to set transverse dispersivities is presented in *Saturated Zone Flow and Transport Process Model Report* (CRWMS M&O 2000bn, Section 3.7.2).

Dispersivities—The dispersion coefficient is a function of dispersivity and flow velocity and determines the rate that the contaminant plume spreads within a medium. Dispersivity has been shown to increase as a function of observation scale, attributed mainly to mixing as more heterogeneities are sampled at larger scales (Gelhar et al. 1992). Field measurements show that the transverse dispersivity is significantly less than longitudinal dispersivity (Fetter 1993, pp. 65 to 66).

In transport simulations, longitudinal dispersion results in earlier arrival but generally lower concentration. Given this behavior, no simple conservative bound exists for the longitudinal dispersion. A distribution consistent with the dispersivity-versus-scale correlation of Neuman (1990) is used in TSPA calculations. Transverse dispersion acts only to reduce concentration, with generally little effect on contaminant breakthrough time.

For comparison with regulations, concentrations are computed by dividing all the mass crossing into the accessible environment by a specified volume of water. For this reason, hydrodynamic dispersion is not expected to play an important role in saturated zone transport simulations at Yucca Mountain.

Decay Chains—The plutonium-239 decay chain (plutonium-239 \rightarrow uranium-235 \rightarrow protactinium-231) is particularly important because the uranium-235 daughter has significantly smaller K_d values compared to its plutonium-239 parent (CRWMS M&O 2000c, Section 3.11.2.6). This decay chain includes only the most important radioactive chain members and omits daughters with short half lives. The neptunium-237 decay chain (neptunium-237 \rightarrow uranium-233 \rightarrow thorium-229) has also been evaluated. The daughter contribution is less than 2 percent at 1 million years (CRWMS M&O 2000ea, Section 6.13.1.2). As such, daughter contributions to neptunium-237 transport are relatively insignificant.

Matrix-Diffusion Coefficients—The effective matrix-diffusion coefficient, which is the product of the molecular diffusion coefficient, tortuosity, and porosity, is used to account for rock geometry effects on matrix diffusion. The matrix diffusion coefficient determines the rate of contaminant flux between the matrix and the fracture. Tortuosity, a measure of deviation from straight flow path through porous medium, is a parameter that reflects the effect of the geometry of the pore structure on the flow within the matrix (it varies between zero and one). The concepts of porosity and molecular diffusion in the matrix are discussed in Section 4.2.9.1.

Experimental data on the tortuosity distribution in the various hydrogeologic units at Yucca Mountain were supplemented by an approach using porosity values to approximate tortuosity (CRWMS M&O 2000ea, Section 6.1.2.4). Tortuosity measurements on devitrified tuffs showed good agreement with this approximation.

Distribution parameters for matrix diffusion coefficients (see Table 4-25 in Section 4.2.8.2.2) are based on the measured diffusion coefficients of tritium and technetium (CRWMS M&O 2000eb, Section 6.6.1.3). The cationic (positively charged and sorbing) radionuclides are assigned values representative of the coefficient for tritium. Based on measured diffusion behavior of cationic radionuclides, this is conservative (CRWMS M&O 2000eb, Section 6.6.1.3). The anionic radionuclides (negatively charged) are assigned values representative of the coefficient for technetium, which (as pertechnetate, the predominant aqueous species of technetium) is approximately 10 times lower than that for tritium. Anionic radionuclides are more likely to be excluded from the matrix pores, which are also negatively charged.

4.2.9.2.4 Sorption

Sorption reactions are chemical reactions that involve the attachment of dissolved chemical constituents to solid surfaces. Although these reactions can be complex in detail, they are typically represented in transport calculations by a constant called the sorption coefficient (CRWMS M&O 2000bn, Section 3.2.4.3).

In the case of the Yucca Mountain flow system, an important performance assessment goal is the prediction of radionuclide transport rates to the receptor location. Radionuclide sorption onto either fracture or matrix surfaces will decrease radionuclide transport rates.

Sorption in Fractured Tuff—Sorption reaction interactions can potentially occur on the surfaces of fractures and within the rock matrix. However, because of a lack of data and to be conservative, sorption on fracture surfaces is neglected, and only sorption within the matrix is included in the saturated zone process models and the TSPA

simulations. For the C-Wells field experiments, analogue tracers were used in place of radionuclides because of environmental considerations. The experiment's reactive tracer, lithium (an analogue for a sorbing radionuclide), was modeled using a matrix-diffusion model with the sorption coefficient of the matrix as an adjustable parameter (CRWMS M&O 2000bn, Section 3.1.3.2). The matrix sorption coefficient that fit the data agreed quite well with the value determined in laboratory sorption tests, thus providing an additional degree of confidence in the matrix-diffusion model. The fact that the early breakthrough of lithium had the same timing as that of the nonsorbing tracers, but with a lower normalized peak concentration, is consistent with matrix diffusion followed by sorption in the matrix.

Transport parameters obtained from the model fits for the saturated zone, with the exception of lithium sorption parameters, are listed in Table 4-28 for the Bullfrog and Prow Pass tuff tests. Further discussion of how these parameters were obtained and how they compare with other studies is provided in *Unsaturated Zone and Saturated Zone Transport Properties (U0100)* (CRWMS M&O 2000eb, Section 6.9).

Lithium sorption parameters were deduced from the field tracer tests. In these tests, lithium sorption always was approximately equal to or greater than

the sorption measured in the laboratory (CRWMS M&O 2000bn, Table 3-5). Details of the methods used to obtain the field lithium sorption parameters and discussions of possible alternative interpretations of the lithium responses are provided in Reimus et al. (1999). Microsphere filtration and detachment rate constants deduced from these tracer tests are provided in *Saturated Zone Colloid-Facilitated Transport* (CRWMS M&O 2000ei, Section 6.1.2).

Experimental sorption coefficients (K_d values) were obtained using rock samples collected from the Topopah Spring welded and Calico Hills nonwelded hydrogeologic units at Busted Butte. The fine particles produced during sample crushing were not removed during the Busted Butte sorption study (CRWMS M&O 2000eb, Section 6.8.5.1.2.2) to duplicate in situ conditions, whereas fine materials were removed in the standard batch-sorption tests. Values for K_d could be influenced by small crushed-rock sizes used for sorption measurement, with the fine materials generating large K_d values. The Busted Butte transport tests are discussed in more detail in *Unsaturated Zone Flow and Transport Model Process Model Report* (CRWMS M&O 2000c, Section 3.11.11.2), *Radionuclide Transport Models Under Ambient Conditions* (CRWMS M&O 2000ea, Section 6.10), and *Unsaturated Zone and Saturated Zone Transport Properties (U0100)* (CRWMS M&O 2000eb, Section 6.8).

Table 4-28. Transport Parameters Deduced from Bullfrog Tuff and the Prow Pass Tuff Tracer Tests

Parameter (units)	Bullfrog Tuff		Prow Pass Tuff
	Pathway 1 ^a	Pathway 2 ^b	
Mass Fraction in Pathway (unitless)	0.12	0.59	0.75
Residence Time, Linear Flow (hr)	37	995	1230
Longitudinal Dispersivity, Linear Flow (m)	5.3	18.8	23.1
Residence Time, Radial Flow (hr)	31	640	620
Longitudinal Dispersivity, Radial Flow (m)	3.6	10.7	6.3
Effective Flow Porosity, Linear ^c (unitless)	0.0029	0.026	0.0068
Effective Flow Porosity, Radial ^c (unitless)	0.0025	0.017	0.0034
Effective Matrix-Diffusion Mass Transfer Coefficient ^d (sec ^{-1/2})	0.00158	0.000458	0.000968

NOTES: ^a Pathway 1 refers to pathways that resulted in the first tracer peak.

^b Pathway 2 refers to pathways that resulted in the second peak.

^c Based on flow log information, it was assumed that 75 percent of the production flow contributed to the Pathway 1 responses and 25 percent of the flow contributed to the Pathway 2 responses.

^d The value of the parameter for pentafluorobenzoate (PFBA) was assumed to be 0.577 times that for bromide.

Source: Adapted from CRWMS M&O 2000eb, Tables 51 and 52.

Sorption data for the saturated zone were also determined during batch experiments, and selected results of those tests are presented in Table 4-29.

Sorption in the Alluvium—In contrast to the fractured tuffs, there are no field-scale tracer transport tests as of yet in the alluvium south of Yucca Mountain to confirm the validity of the sorption coefficient data. Tracer testing activities are underway in the Alluvium Testing Complex. However, transport of sorbing solutes in porous media not controlled by fractures has been well studied (CRWMS M&O 2000bn, Section 3.2.4.3), and it is reasonable to assume that the transport velocities of sorbing radionuclides in the alluvium can be conservatively represented using an equilibrium sorption coefficient. Sorption onto alluvium from the Nye County Early Warning Drilling Program wells has been measured for a few key radionuclides (CRWMS M&O 2000eb, Section

6.4.5). For the remaining radionuclides, sorption coefficients are estimated based on values measured for crushed tuff (CRWMS M&O 2000eb, Section 6.9.3.3).

4.2.9.2.5 Colloid-Facilitated Transport

Colloid-Facilitated Transport Experiments—

Figure 4-136 provides a conceptual illustration of colloid-facilitated transport processes. Colloids in the saturated zone are capable of facilitating the transport of radionuclides over long distances if (1) a large percentage of the colloids do not irreversibly filter or attach to surfaces of subsurface materials and (2) radionuclide desorption rates from the colloids are slow (i.e., radionuclides are strongly sorbed to colloids), or if (3) colloid concentrations are so high that colloid surfaces can effectively compete with immobile surfaces for radionuclides. However, analyses of colloid

Table 4-29. Sorption-Coefficient Distributions for Saturated Zone Units From Laboratory Batch Tests

Element	Rock Type	K_d (mL/g)			
		Minimum	Maximum	Mean	Coefficient of Variation
Americium	Devitrified	100	2000	N/A	N/A
	Vitric	100	1000	400	0.20
	Zeolitic	100	1000	N/A	N/A
	Iron oxide	1000	5000	N/A	N/A
Neptunium	Devitrified	0	2.0	0.5	0.3
	Vitric	0	2.0	0.5	1.0
	Zeolitic	0	5.0	1.0	0.25
	Iron oxide	500	1000	N/A	N/A
	Alluvium	0	100	18	1.0
Plutonium	Devitrified	5	100	50	0.15
	Vitric	50	300	100	0.15
	Zeolitic	50	400	100	0.15
	Iron oxide	1000	5000	N/A	N/A
Uranium	Devitrified	0	5.0	N/A	N/A
	Vitric	0	4.0	N/A	N/A
	Zeolitic	5	20.0	7.0	0.3
	Iron oxide	100	1000	N/A	N/A
	Alluvium	0	8.0	N/A	N/A
Chlorine, Technetium, Iodine	All tuffs	0	0	N/A	N/A
Technetium	Alluvium	0.27	0.62	N/A	N/A

NOTES: N/A = not applicable. Source: CRWMS M&O 2000eb, Table 2b.

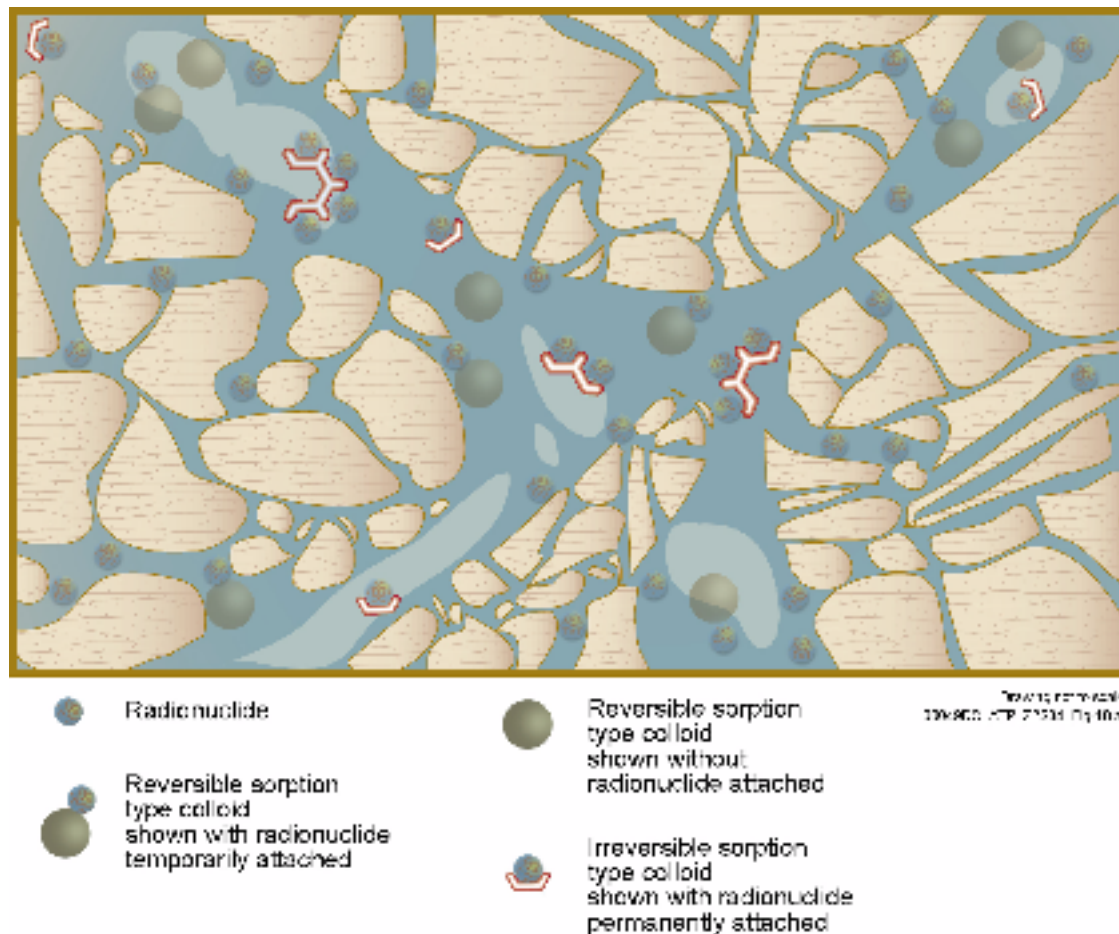


Figure 4-136. Colloid-Facilitated Transport

Colloids are small particles ranging from 0.1 to 5 μm (0.000004 to 0.0002 in.) in diameter. Some radionuclides are sorbed to colloids and thereby transported in groundwater. Source: CRWMS M&O 2000a, Figure 3.7-6.

concentrations and size distributions in Yucca Mountain groundwater have not found high concentrations of colloids. Published correlations of colloid concentrations as a function of water chemistry, which draw upon a global database of measurements, also suggest that colloid concentrations are unlikely to be high enough for the third condition to be met even under perturbed conditions (Triay, Degueudre et al. 1996).

The DOE has addressed the filtering or attachment of colloids to surfaces of subsurface materials using polystyrene microsphere data from the C-Wells field tests to obtain conservative estimates of colloid attachment and detachment rates in frac-

tured tuffs. The DOE also has used published data to obtain bounding estimates of attachment and detachment rates in alluvium (CRWMS M&O 2000bn, Section 3.2.4.5.3). The published correlations of colloid concentrations as a function of water chemistry also support indirect estimates of attachment rates, as it is widely accepted that lower concentrations occur under conditions in which colloids are less stable and, hence, more likely to attach to surfaces. Details of stability-based arguments for bounding colloid concentrations and attachment rates in Yucca Mountain waters are provided in *Colloid-Associated Radionuclide Concentration Limits: ANL* (CRWMS M&O 2000dt, Section 6).